



S2 MPC

Copernicus Sentinel-2 GRI as Database of GCPs in L1B & L1C - Product Handbook

Ref. S2-MPC_PHB_GCP_L1B_L1C_GRI



Authors Table

	Name	Company	Responsibility	Date	Signature
Written by	GRI Team	CS	S2 GRI Team	2023-07-07	
Verified by	O Devignot	CS	Quality Manager	2023-07-07	
Approved by	L. Pessiot	CS	Service Manager	2023-07-07	

Change Log

Issue	Date	Reason for change	Pages(s)/Section(s)
V1	2023-05-31	Creation	
V2	2023-06-26	Update crossvalidation with corrected tools taking into account that several datastrips are duplicated	§5.3.2: Consistency with Multi-Layer L1B & L1C GRI
V3	2023-07-07	Update of the document title	

Table of contents

1. INTRODUCTION	5
1.1 Purpose of the document	6
1.2 References	7
1.3 Terminology	7
2. PRODUCTS SPECIFICATIONS	8
2.1 Main objectives	8
2.2 Technical requirements	8
2.2.1 Spatial distribution	8
2.2.2 GCPs chips	8
3. PRODUCT FORMAT	10
3.1 L1B & L1C GCP GRI organisation	10
3.1.1 Tiling	10
3.1.2 Content	10
3.1.2.1 L1B GCP GRI content	10
3.1.2.2 L1C GCP GRI content	10
3.2 Chips description	11
3.3 GCP Naming convention	11
3.4 A json file per 1°x1° square area	12
4. PRODUCT GENERATION AND EDITING PROCESS	14
4.1 Extraction of GCPs	14
4.1.1 Extracting candidates of interest from the GRI	14
4.1.2 Validating the candidates with S2 L1C images	14
4.2 Handling overlaps and Filtering	16
4.2.1 Multiple GRI observations	16
4.2.2 Spatial Filtering	16
4.2.3 Exclusion of measurements with no-data in the chip file	16
4.3 Coordinates processing and chips generation	17
4.4 Visual checking in critical areas of the GCPs DB	17
4.5 Addition of quality scores	18
4.5.1 Absolute Planimetric Accuracy	18
4.5.2 Relative accuracy	18
4.5.3 Clouds, snow, and water statistics	19
4.5.4 Seasonal Correlation and Curvature scores of each GCP	20
4.5.5 GCP Radiometric assessment indexes	20
4.5.6 Final Quality Score	21
4.6 Final Validation	22
4.7 Splitting in two products	22
5. PRODUCT QUALITY PERFORMANCE	23
5.1 Known issues or supposed weaknesses	23
5.2 Coverage and density	23

5.2.1	Global coverage.....	23
5.2.1.1	Europe	27
5.2.1.2	Africa	28
5.2.1.3	North America	31
5.2.1.4	South America.....	32
5.2.1.5	Asia	35
5.2.1.6	Australia.....	36
5.2.1.7	Antarctica	38
5.2.2	Number of chips per GCP	39
5.3	Geolocation performance	39
5.3.1	Absolute planimetric accuracy	39
5.3.2	Consistency with Multi-Layer L1B & L1C GRI	40
5.3.2.1	Absolute coherence with Multi-Layer L1C GRI.....	40
5.3.2.2	Relative coherence with Multi-Layer L1C GRI.....	41
5.4	GCPs Correlation performance	42
5.4.1	Seasonal correlation	42
5.4.1.1	Europe	43
5.4.1.2	Africa	46
5.4.1.3	North America	47
5.4.1.4	South America.....	49
5.4.1.5	Asia	50
5.4.1.6	Australia.....	51
5.4.1.7	Antarctica	53
5.4.2	Final Score	53
5.4.2.1	Europe	55
5.4.2.2	Africa	56
5.4.2.3	North America	58
5.4.2.4	South America.....	59
5.4.2.5	Asia	62
5.4.2.6	Australia.....	63
5.4.2.7	Antarctica	64
5.5	GCPs Radiometric quality performance	65
6.	USER GUIDE	66
6.1	Recommendations of use	66
6.2	Examples of use.....	66
6.2.1	Use of the L1C GCP GRI by the Sentinel-2 Level-1 processor	66
6.2.2	Estimation of the geometrical accuracy of S2 (or other sensors images)	67
7.	DISTRIBUTION, LICENSE, AND COPYRIGHTS	68
7.1	Distribution.....	68
7.2	License and copyrights	68

1. Introduction

The Multi-Layer-L1B Global Reference Image (GRI) is a layer of reference composed of Sentinel-2 mono-spectral (B04, red band) L1B Datastrips accurately geolocated (top map of Figure 1 above). The GRI covers most emerged land masses except Antarctica and has a global geolocation uncertainty better than 6 m. It is currently used to refine the Copernicus Sentinel-2 imagery. The geometric refinement for Sentinel-2 products was first deployed over the Euro-Africa region (March 2021) and then in August 2021 worldwide. Results of this activation were an improved multi-temporal co-registration and absolute geolocation accuracy of the Sentinel 2 products.

The benefit of using the Sentinel-2 GRI has been recognized as also applicable to other satellite data than S2, and in general as a very good product to improve the geolocation.

However, as it was initially created for internal use in the Sentinel-2 mission, the Multi-Layer L1B GRI is not very easy to handle and this makes it usable only by expert users.

In this framework, the conversion of the Multi-Layer L1B GRI as Database of GCPs has been identified as an important improvement (bottom map of Figure 1 above).

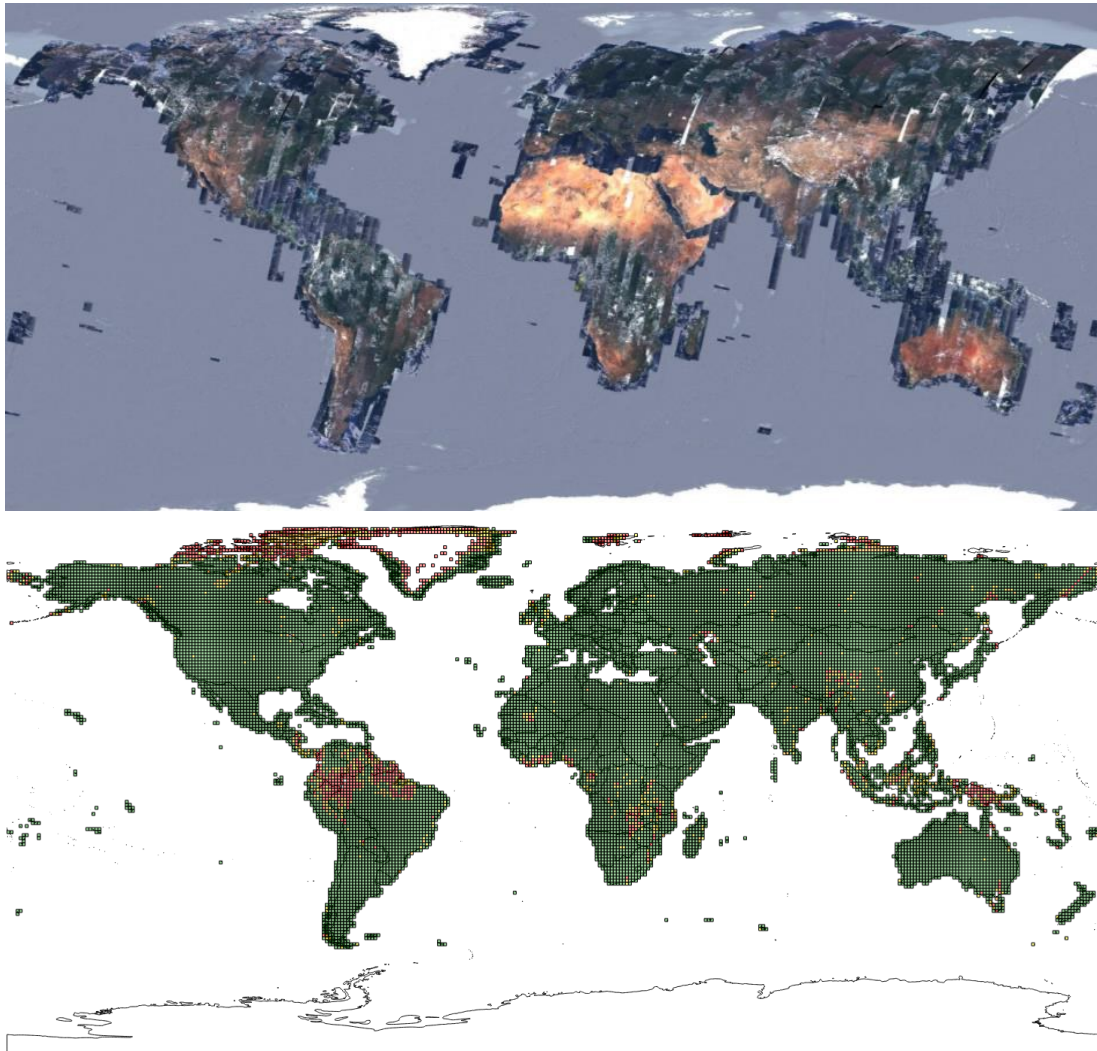


Figure 1: From the Multi-Layer L1B GRI (top) to the L1B & L1C GCP GRI (bottom)

The first map represents the coverage (composed of datastrips) of the Multi-Layer L1B GRI from which the L1B & GCP GRI are extracted, while the second map represents the coverage of the L1B & L1C GCP GRI (composed of square degrees).

1.1 Purpose of the document

This Product Handbook aims at providing in a unique document, all the information regarding the generation and the use of the Sentinel-2 Global Reference Image (GRI) in L1B & L1C GCP format.

Please note that the GRI products and related documentation are full, free and open for the international users.

1.2 References

Id	Title	Reference
[VAL-L1B-L1C-GCP]	Sentinel-2 L1B & L1C GCP GRI Validation Report	S2-MPC_VAL_GCP_L1B_L1C_GRI_V1
[PHB-ML-L1B-GRI]	Sentinel-2 Multi-Layer L1B GRI Validation Report	S2-MPC_PHB_ML_L1B_GRI_V1

All the above documents are available on Sentinel Online website in the Sentinel 2 Document Library: <https://sentinels.copernicus.eu/web/sentinel/user-guides/sentinel-2-msi/document-library>.

1.3 Terminology

Datastrip	Within a given Sentinel-2 Datatake, a portion of sensed image downlinked during a pass to a given station is termed Datastrip. If a particular orbit is acquired by more than one station, a Datatake is composed of one or more Datastrips (for more details see [S2-PSD])
DEM	Digital Elevation Model
Datatake	Continuous acquisition of an image from one Sentinel-2 satellite in a given MSI imaging mode (for more details see [S2-PSD])
GCP	Ground Control Point
GRI	Ground Reference Image
MGRS	Military Grid Reference System ¹ : Tiling system on which the Sentinel-2 tiling system is aligned with.
Tile (S2 L1C)	110 km ² ortho-images in UTM/WGS84 projection. Earth is subdivided on a predefined set of tiles, defined in UTM/WGS84 projection and using a 100 km step. However, each tile has a surface of 110x110km ² in order to provide large overlap with the neighbouring (for more details see [S2-PSD])

¹ https://en.wikipedia.org/wiki/Military_Grid_Reference_System

2. Products Specifications

2.1 Main objectives

The L1B & L1C GCPs DB are built to answer to the following purposes:

- They shall at least have the same geometric performance as the Multi-Layer L1B GRI.
- ✓ They shall be easy to be handled by the S2 Level-1 processor.
- ✓ They shall have a data format easy to understand to support the processing of Sentinel-2 data by the operational processor with special attention on time performance optimization.
- ✓ They shall be shaped in such a way to be easily accessible by the international user community.
- ✓ They shall have a global coverage, i.e. cover all the continents (same coverage as the Multi-Layer L1B GRI).
- ✓ They shall be usable also for satellite data with lower spatial resolution (up to 50 m).
- ✓ They shall be generated using the 30 m Copernicus DEM.

2.2 Technical requirements

Furthermore, to address the operational requirements of the S2 mission and potentially other missions, the technical requirements of the GCPs have been defined as in the following two sections.

2.2.1 Spatial distribution

The DB coverage corresponds to the GRI coverage, excluding water areas. It offers a worldwide coverage including many isolated islands.

The requirements on the density are described by square degrees (deg^2):

- ✓ the maximum density within a tile should not exceed 400 pts / deg^2
- ✓ the average density of the tiles should be at least 200 pts / deg^2
- ✓ at least 70% of the tiles should have a density ≥ 200 pts / deg^2
- ✓ at most 10 % of the tiles should have a density between 100 and 200 pts / deg^2
- ✓ a best effort shall be brought for the remaining tiles.

2.2.2 GCPs chips

Each of the databases is a set of chip images extracted from the Multi-Layer L1B GRI.

The chips are provided in GEOTIFF format, 16 bits, 57px x 57px at 10m of resolution.

As the Multi-Layer L1B GRI products, it contains only the Sentinel-2 B04 band (red band). The associated coordinates (sensor or ground) correspond to the centre of the chip.

L1C images are orthorectified using the 30 m Copernicus DEM at constant Z.

3. Product Format

This section provides details about the L1B & L1C GCP GRI formats and content.

3.1 L1B & L1C GCP GRI organisation

3.1.1 Tiling

The data are delivered by tiles of $1^\circ \times 1^\circ$, where the name of each tile is given by the lower left corner.

The naming convention is [NS]YY[EW]XXX, with:

- ✓ [NS]: North or South hemisphere
- ✓ YY: absolute value of the longitude
- ✓ [EW]: East or West of Greenwich meridian
- ✓ XXX: absolute value of the latitude

The L1B & L1C GCP GRI are both composed of 17836 square degrees.

Both L1B & L1C GCP GRI contain the same GCP, only their format differs from L1B and L1C GCP GRI.

3.1.2 Content

3.1.2.1 L1B GCP GRI content

For each square degree:

- ✓ the L1B chips are in the ./L1B_chips folder.
- ✓ a single .json file gathering all the GCPs.

L1B chip files are in TIF format and in sensor geometry.

In parallel to the square degrees, the metadata of the Multi-Layer L1B GRI DS are provided to be able to rebuild the L1B geometric model of the DS.

These data being quite large and common to many GCP and square degrees, they are provided apart from the square degrees. In the json file of each square degree, a link to the DS Metadata file can be found for each GCP chip. This allows users to download or not the metadata they are interested in.

3.1.2.2 L1C GCP GRI content

For each square degree:

- ✓ the L1C chips are in the ./L1C_chips folder.
- ✓ a single .json file gathering all the GCPs.

L1C chip files are in TIFF format and in ground geometry.

3.2 Chips description

The chip images size is of 57*57 pixels at 10 m of resolution, i.e. 570*570 meters. The chip files are provided in GeoTIFF format.

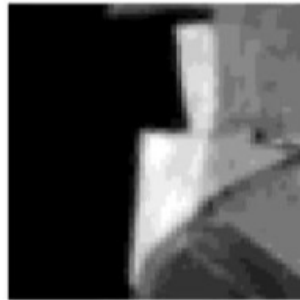


Figure 2: Example of L1C chip, 57*57 pixels i.e. 570*570 m

Ground coordinates are rounded at $10^{-2} \text{ m} = 10^{-7}^\circ$, i.e. for a precision of 10-2 m. The associated coordinates (sensor or ground) correspond to the centre of the chip.

L1C images are locally rectified in UTM projection at constant Z, in line with the name of the point. Phasing with L1C product is ensured.

3.3 GCP Naming convention

The GCPs are named with respect to

[MGRS]_[0-9]{4}

Where:

- ✓ **MGRS** is the name of the tile, in MGRS format, where the point was projected
- ✓ **[0-9]{4}** is a unique number to ensure unicity of the name of the point.

Example: 32TLP_1608

The different measures (i.e. occurrences, i.e. chips) of the same GCP respect the following convention:

[GCP name]_[0-9]{2}

With:

- ✓ **[0-9]{2}** is a number indicating the observation number.
 When there is no overlap, there is only measurement #00, when there is an overlap of 2, there are measurements #00 and #01 etc.

Examples: 32TLP_1608_00 as major measure, 32TLP_1608_01, 32TLP_1608_02 minor ones.

Chip images filenames are in line with the naming convention and stored in "L1B_chips" folder for L1B GCP GRI and "L1C_chips" folder for L1C GCP GRI.

3.4 A json file per 1°x1° square area

Per folder, i.e. per square degree, a json file contains all the metadata associated with up to 400 GCPs.

We describe here the main fields available in the json metadata:

- ✓ The header tags "**Product_Info**" & "**Tile_Info**":
 The header for each json file contains properties applicable to the entire GCPs included in the square degree.
 - ✎ **Version**: the GCP DB version
 - ✎ **Z_Source**: the DEM source
 - ✎ **Ellipsoid_Name**: the reference ellipsoid
 - ✎ **Geoid_Name**: the reference geoid
 and
 - ✎ **Tile_Name**: the name of the 1°x1° square, typically NXXEXXX
 - ✎ **Tile_Extent**: the geographical extension in degrees of the 1°x1° square
 - ✎ **Planimetric_Accuracy**: ellipsoid value and unit ("None" if not available)
 - ✎ **DEM_Accuracy**: Z accuracy value and unit
 - ✎ **Number_of_GCP**: number of GCP in the square degree
- ✓ Then for each GCP,
 - ✎ "**ID**" tag, the ID of the GCP (see the description in section 3.3).
 - ✎ "**GCP_Info**" tag
 Contains information on the GCP position in lon, lat and Z and the related accuracy measurements, i.e.:
 - "**Longitude**": longitude in degrees of the centre of the GCP (precision 10⁻² m)
 - "**Latitude**": latitude in degrees of the centre of the GCP (precision 10⁻² m)
 - "**EPSG**": EPSG code between 1024–32767,
 - "**X**" and "**Y**": ground coordinates of GCP centre, X and Y position in meters (UTM)
 - "**MGRS_Tiles**": list of the S2 tiles into which the GCP centre falls,
 - "**Altimetry**": Z value and unit,
 - "**Ellipsoid_Value**": height above ellipsoid value,

- ↗ **"Radiometry"** tag

Contains the statistical indicators, assessment of the radiometry for each GCP:

 - **"Y_Gradient_Sums"**: first and second order integrated gradients over the GCP in Y (see the description in section 4.5.5).
 - **"X_Gradient_Sums"**: first and second order integrated gradients over the GCP in X (see the description in section 4.5.5).
 - **"Anisotropic_Ratio"**: ratio of anisotropy of the GCP, measures its dependency to the rotation (see the description in section 4.5.5).
 - **"Entropy"**: Shannon entropy (see the description in section 4.5.5).
 - **"Masks_CL_CLS_WA_SN"**: for each GCP occurrence, the [clouds, cloud shadows, water and snow] coverages in % are calculated using the corresponding S2 L1C tile and the Fmask 0.5.5 software (see the description in section 4.5.3).
- ↗ **"Relative_Accuracy"**: relative coherence of the measurements, only available when a GCP has several measures (i.e several chips) (see the description in section 4.5.2).
- ↗ **"Quality_Indicators"** tag
 - **"Quality_Score"**: integrated quality score (see the description in section 4.5.6).
 - **"Seasonal_Correlation_Scores"**: seasonal correlation scores computed for each chip of the GCP. Summer season is considered from April to September, while the winter season from October to March (see the description in section 4.5.4).
 - **"Seasonal_Curvature_Scores"**: seasonal curvature scores computed for each chip of the GCP (see the description in section 4.5.4).
- ✓ **"GRI_List"** tag: list of the measurements, i.e. the GCP occurrences (chips), extracted from the Multi-Layer L1B GRI.
- ↗ **"GRI_Measure"** tag: for each GRI_Measure, the tag describes one occurrence of the GCP. This tag is thus replicated for each GCP occurrence.
 - **"Product_Name"**: name of the Multi-Layer L1B GRI product from which the GCP is taken,
 - **"Datastrip_Name"**: name of the Multi-Layer L1B GRI datastrip from which the GCP is taken,
 - **"S2_Detector"**: S2 detector number from which the GCP is observed
 - **"Chips"**: Chip description

For L1B GCP this tag contains:

 - **"Image_Coordinates"**: coordinates of the centre of the chip in L1B pixels in the DS
 - **"Chip_File"**: L1B chip file (57*57 pixels in geotiff format)
 - **"MTD_File"**: link to a compressed file containing the metadata and the auxiliary data of the DS from which the chip has been extracted.

For L1C GCP this tag contains:

 - **"Chip_File"**: L1C chip file (57*57 pixels in geotiff format)
- ↗ **"Validation_L1C_List"** tag:
 - **"Product_Name"**: list of S2 tiles used for the validation, each tile identified by "Tile, Date, Rel orbit"

4. Product Generation and Editing process

The generation of the L1B & L1C GCP GRI has been done in several steps:

- ✓ Extraction of GCP candidates from the Multi-Layer L1B GRI,
- ✓ Handling overlaps and Filtering,
- ✓ Coordinates processing,
- ✓ Chips generation,
- ✓ Visual checking in critical areas,
- ✓ Addition of quality scores,
- ✓ Final validation,
- ✓ Splitting in two distinct products (L1B & L1C).

Each of these steps is detailed in the following sections.

4.1 Extraction of GCPs

The L1B & L1C GCPs GRI are built from the Multi-Layer L1B GRI. It means that the GCPs are extracted from this "historical" GRI.

The extraction of the GCPs was made in 2 main steps:

- ✓ extraction of textured points within the images (candidates),
- ✓ validation of the candidates on a S2 L1C stack.

4.1.1 Extracting candidates of interest from the GRI

The first task of the workflow chain was to extract textured features of the landscape within the Multi-Layer L1B GRI images. This task was made in L1B sensor geometry and was achieved using the Hessian criteria within the images. This criterion provides local maxima that can be considered as textured points. A special care was dedicated to the distribution within the image, to ensure points everywhere within the L1B datastrip. This method provides textured points but does not ensure the relevancy of the detail. Indeed, it could include many clouds since these are also textured. A filtering effort had thus to be made onto these numerous candidates to become valid GCPs.

4.1.2 Validating the candidates with S2 L1C images

This task consisted in validating or rejecting the extracted features of previous task. Each feature was checked based on its correlation with several cloud free images extracted from the whole S2 archive. The more the correlations of the feature with the stack were successful, the more the point could be trusted. When the correlation always failed, the feature was rejected.

For this the L1B candidates were converted into L1C chips and then the correlation was done on a L1C S2 stack.

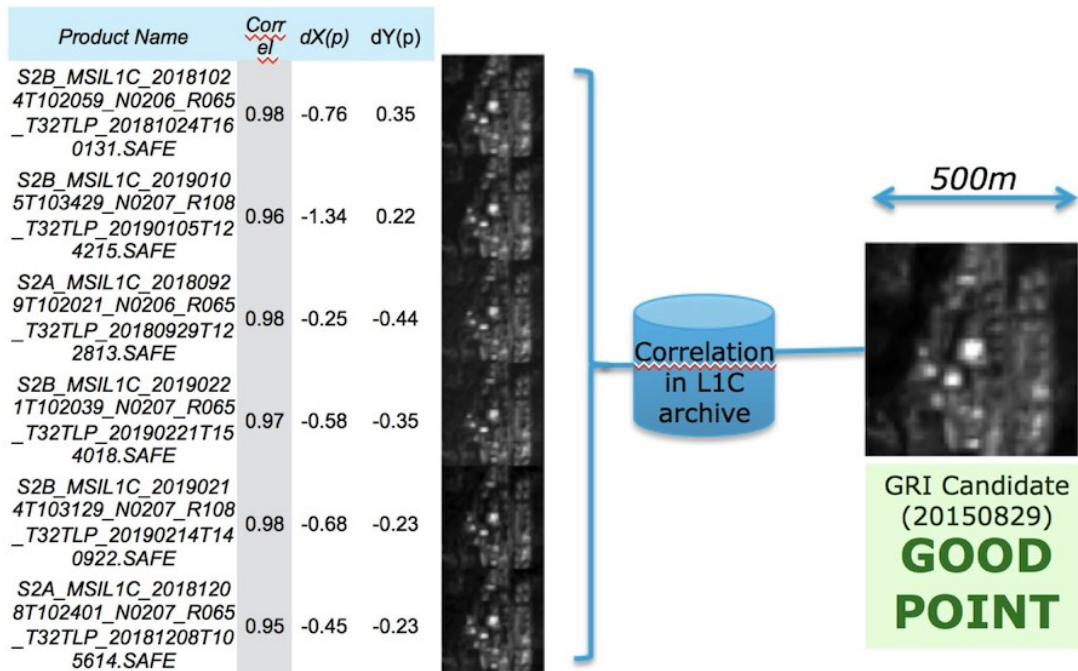


Figure 3: Example of a valid candidate

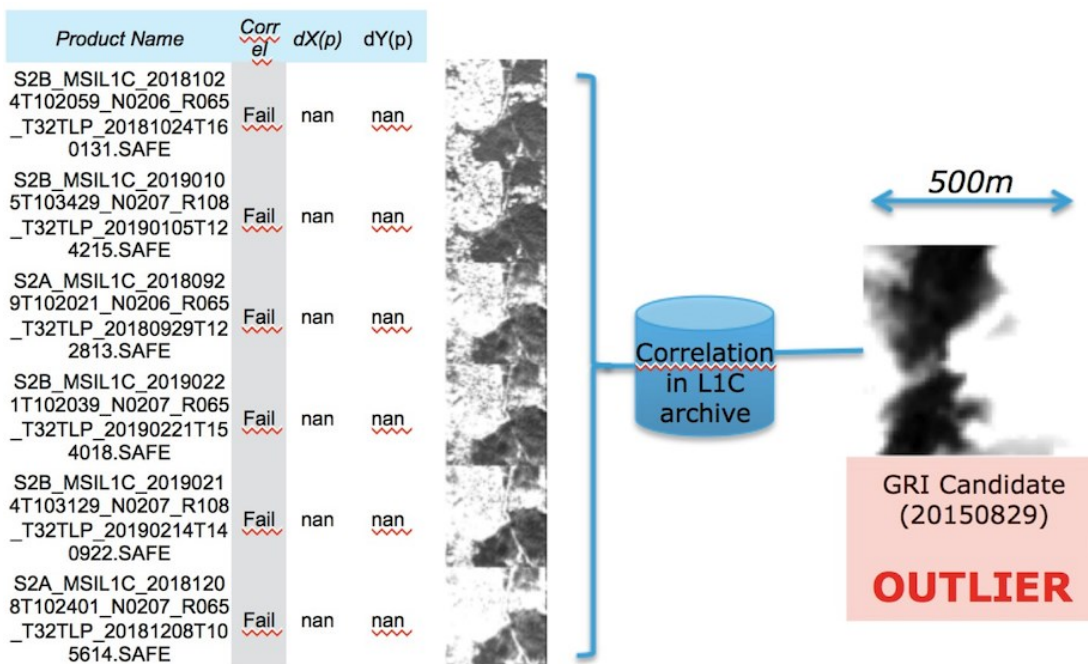


Figure 4: Example of a rejected candidate due to cloud coverage

The stack of S2 L1C products used to validate the candidates is mainly from 2018 and 2019. For every MGRS tile, the images were selected as much as possible from all the corresponding relative orbits. Consequently, the « thickness » of the stack increases with the latitude.

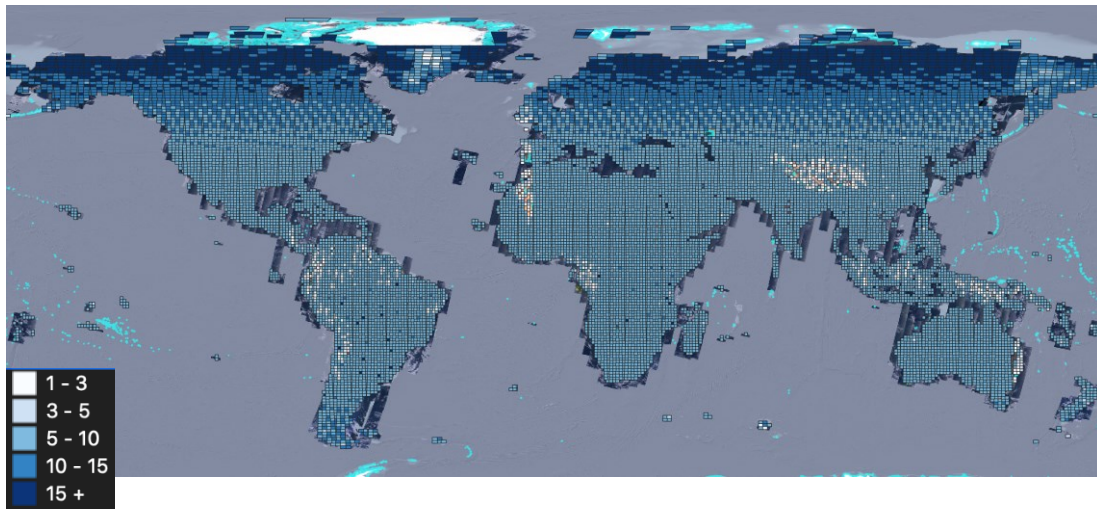


Figure 5: Number of S2 tiles contained in the stack used for validation

4.2 Handling overlaps and Filtering

4.2.1 Multiple GRI observations

At this step, the GCPs were considered as single measurement. Since the Multi-Layer L1B GRI contains overlapped areas, it was interesting to take this advantage into account. That's why overlapping images were retrieved from the GRI to extract the corresponding measurements. Each GCP is consequently composed by 1 major measurement + n minor measurements (regarding the overlap) called chips. All the chips were correlated with the major one to avoid clouds within the minor measurements. All the possible overlaps were considered, independently from the relative orbit, to provide different angles of views of the same detail of the landscape.

4.2.2 Spatial Filtering

All GCPs within a distance of 30 m were considered as duplication. When several points are found, only one of them was kept.

A spatial filtering was processed for tiles over 400 pt/deg² to ensure a good spatial distribution. It consisted in dividing the tiles in clusters (50 clusters by square degree with kmeans2 algorithm) and keeping 8 points by cluster with the best quality index.

4.2.3 Exclusion of measurements with no-data in the chip file

All measurements near L1B datastrip border (i.e column image coordinate < chip_size/2 or > detector_size - chip_size/2) were deleted to avoid black data in the final chips (with detector_size = 2552 pixels and chip_size = 57 pixels).

4.3 Coordinates processing and chips generation

For each GCP, the major measurement was kept as reference to compute the ground coordinate using the 30 m Copernicus DEM. This ground coordinate was converted in local UTM coordinate and rounded to L1C grid. This L1C phased ground coordinate became GCP coordinate and all measurements and chips were reprocessed.

L1B chips were produced by bicubic resampling on the original L1B GRI product and centred on the image measurement (57x57 pixels). L1C chips were produced by rectifying L1B chip at constant Z, centred on UTM point coordinates (57x57 pixels, 10 m resolution).

4.4 Visual checking in critical areas of the GCPs DB

When the minimal density is not reached, it is important to provide points which are guaranteed to be correct (e.g. not cloudy points). Consequently, these specific areas have been visually checked by operators, and square degrees tiles were flagged as visually checked.

Square degree tiles were checked by an operator when:

- ✓ The tile had less than 10 pts (independently from the land surface): 821 tiles (red tiles in Figure 6)
- ✓ The tile had less than 80 pts (related to real land surface): 520 tiles (yellow tiles in Figure 6)

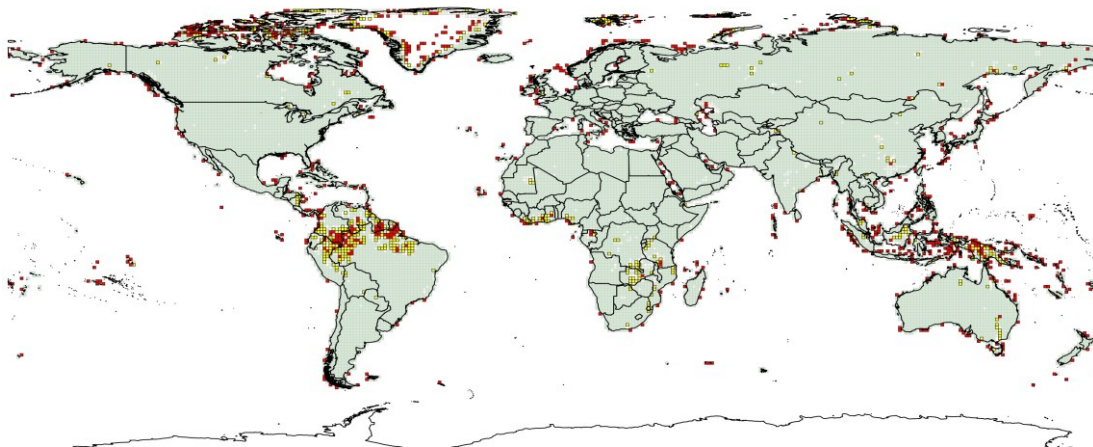


Figure 6: Areas visually checked by an operator

All the GCPs for which the visual check showed that the GCP is finally not usable have been removed from the database.

The GCPs that have been checked by an operator are flagged as valid/invalid.

4.5 Addition of quality scores

This step consists in assessing the GCPs quality and providing some quality scores for each square degree and GCP. These scores are available in the json metadata file of each square degree.

4.5.1 Absolute Planimetric Accuracy

The absolute planimetric accuracy is directly related to the accuracy of the Multi-Layer L1B GRI (see Multi-Layer L1B GRI documentation for further information).

This value is provided for each square degree.

When some values were missing to compute the accuracy, no value is given. The accuracy is finally provided as a class of accuracy from 1 to 4 with respect to the following table.

Table 1: Planimetric accuracy classes

Requirement	Class	Value
no value	NA	NA
< 7m	1	0 – 7
< 9m	2	7 – 9
< 12.5m	3	9 – 12.5
>= 12.5m	4	>= 12.5

Considering L1C chip, the absolute planimetric accuracy takes also into account the DEM accuracy, as expressed in the following formula:

$$\text{AbsoluteAccuracy} = \sqrt{\sigma(\text{AC}_{\text{GRI}})^2 + \sigma(\text{DEM})^2 \cdot \tan(i)^2}$$

Where:

- ✓ $\sigma(\text{AC}_{\text{GRI}})$: absolute accuracy computed for the Multi-Layer L1B GRI per square degree,
- ✓ $\sigma(\text{DEM})$: 30 m Copernicus DEM uncertainty, taken from the DEM tile metadata for the square degree,
- ✓ i : incidence angle in the centre of the square.

4.5.2 Relative accuracy

The relative accuracy of the measurements is estimated when there is an overlap within a GCP, i.e. several chips for one GCP. It provides information on the relative coherence between the L1C chips. It is related to the relative coherence of the GRI between the products, the DEM accuracy and the angle of acquisition (range = [-10.2°, +10.2°] in roll).

The relative accuracy is expressed as:

$$\text{RelativeAccuracy} = \sqrt{\sigma(RC_{GRI})^2 + \sigma(DEM)^2 \cdot \tan(i)^2}$$

Where:

- ✓ $\sigma(RC_{GRI})$: relative planimetric accuracy computed for Multi-Layer L1B GRI per square degree,
- ✓ $\sigma(DEM)$: 30 m Copernicus DEM uncertainty,
- ✓ i : incidence angle in the centre of the square.

This information is finally provided as a class value in the final product.

The DEM accuracy is also provided, extracted from the Copernicus 30 m DEM metadata. When the information is missing in the DEM, the value is "NS".

As for the planimetric accuracy this information is provided as a class value from 1 to 4.

Table 2: Relative coherence classes

Requirement	Class	Value
no value	NA	NA
< 1m	1	0 - 1
< 3m	2	1 - 3
< 5m	3	3 - 5
>= 5m	4	>= 5

4.5.3 Clouds, snow, and water statistics

As the GCPs are extracted from the Multi-Layer L1B GRI, some of them can still contain clouds, snow or water as the initial Multi-Layer L1B GRI also contains cloudy images, despite the previous processing chain.

Each GCP is thus provided with statistics for clouds, clouds shadows, water and snow percent coverage computed with the Fmask 0.5.5 Python software ².

Please note that these statistics are provided to the user informatively for each GCP. The GCPs are not filtered according to these statistics letting the users free to decide which GCP can be useful for their own usage and therefore perform their own filtering.

² https://www.pythonfmask.org/en/latest/fmask_fmasc.html

4.5.4 Seasonal Correlation and Curvature scores of each GCP

In order to maximize the potential for image correlation, the GCP must, as much as possible, be robust to the changes in the seasonality and time. It must be also noticed that most of the images used in the Multi-Layer L1B GRI were acquired between 2015 and 2016. Since that time the surface may have changed.

To ensure that the GRI database is up-to-date for the operational requirements of S2, 4 recent S2 images have been used to validate each GCP. Specifically, the period from September 2021 to September 2022 has been selected for this purpose.

To estimate the seasonal potential of correlation for each GCP, a bi-bicubic optimized correlator was used to provide sub-pixel estimates of the spatial shifts between the GCPs (the reference), and the selected images (recent S2 acquisition). Around the maximum shift found with bicubic interpolation, the curvature was also computed using a quadratic fit.

For this seasonal correlation assessment, two "seasons" are considered:

1. Summer: from April to September
2. Winter: from October to March.

4.5.5 GCP Radiometric assessment indexes

The computation of the radiometric indexes aims at providing the information needed to verify that each GCP includes strong gradients, enough texture, and sufficient anisotropy.

The assessment of the GCPs for the detection of a local spatial shift in X and Y or to a potential rotation (typically in case of the use with another sensor) is performed with the estimation of some radiometric quality indicators for each GCPs, namely:

- ✓ The (normalised specific) **Shannon Entropy**:

It is estimated using the GCP image chip.

Entropy measurement is an indicator of the texture of the GCP: a large entropy is an indicator of a good GCP as it will be seen easily from the background.

Entropy estimation is performed using the SciPy related 'Entropy' functions and the formulation is:

$$E = -\sum_{B04=1}^{B04=nval} P(B04=i) * \log(P(B04=i)) / \log(nval)$$

[Nota] The normalised specific entropy is used here as a value between [0,1].

- ✓ **First and second order sum of gradients in X and Y directions:**

First order is the simple calculation using Sobel filter of both gradient sums in X and Y directions over the GCP. Second order is the simple calculation of both gradient sums in X and Y directions over the first order gradient.

✓ The **anisotropy ratio**:

The anisotropy ratio assesses the robustness to the rotation of the GCP. A low anisotropy ratio, close to 0, indicates typically a strong dependence of the GCP to a potential rotation (and inversely). The anisotropy ratio is estimated using an empirical semi-variogram exponential model of the local covariance:

$$\gamma(\Delta x, \Delta y) = \sigma^2 + \sigma^2(1 - \exp(-\Delta L(\theta)))$$

With the elliptical model to be adjusted onto the estimated semi-variogram:

$$L(\theta) = L_{min}L_{max}\sqrt{L_{max}^2\cos^2(\theta-\varphi) + L_{min}^2\sin^2(\theta-\varphi)}$$

The anisotropic ratio is thus defined for each GCP as:

$$R_{aniso} = L_{min}/L_{max}$$

L_{min} and L_{max} parameters (see Figure 7) of the elliptical models, are fitted onto the experimental semi-variogram using a Level-set approach (David, 2004).

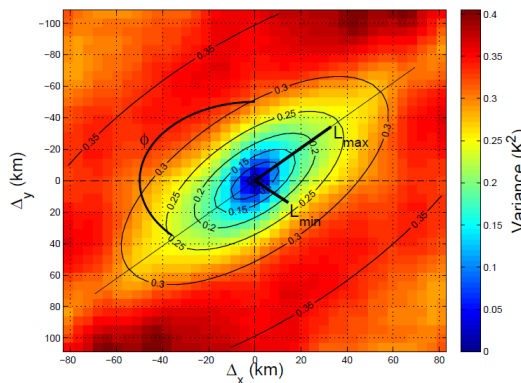


Figure 7: The adjustment of the elliptical model onto the empirical semi variogram model to estimate the anisotropy ratio

4.5.6 Final Quality Score

A final integrated Quality Score (QS) is computed for each GCP.

The correlation and curvature scores are commonly used to evaluate the quality and accuracy of the extracted GCPs.

The final score, provides an overall assessment of the performance of the GCPs.

The table below shows how the final scores are computed depending on the values of the seasonal correlation and curvature scores.

Table 3: Final Quality Score computation

Corr. \ Curv.	≥ 0.9	0.9-0.8	0.8-0.6	< 0.6
≥ 0.1	1	2	3	5
0.1-0.05	2	3	4	5
< 0.05	3	4	5	5

Where:

- ✓ Corr: average of all seasonal correlations.
- ✓ Curv: average of all curvatures.

For instance, for a GCP, if the correlation score computed (Corr) is equal to 0.88 and the curvature score (Curr) 0.04, the final score will be 2 as shown in above table.

4.6 Final Validation

The final validation has been made by comparing the GCP in L1C format with the Multi-Layer L1C GRI in order to verify that they are consistent.

The L1C GCP GRI and the Multi-Layer L1C GRI have the same origin and thus have the same extend. However, as these GRI (i.e. Multi-Layer L1C and L1C GCP) have been generated based on two different methods, they could be cross-validated.

They are thus expected to both have the same quality than the Multi-Layer L1B GRI and shall be consistent between them. A mean shift by tile regarding all GCP over it is computed for all L1C Tiles of the Multi-Layer L1C GRI.

4.7 Splitting in two products

In order to have two distinct products (L1B GCP GRI and L1C GCP GRI), the last step consisted in creating two different products only keeping in each product the relevant set of metadata in the json file and the relevant set of tiles for each product.

5. Product Quality Performance

This section provides the main synthetic indicators of the quality performance of the L1B & L1C GCP GRI.

Please note that most of the results are detailed for each of the following geographical areas:

- ✓ Europe: this area doesn't strictly include Europe countries, as the Russian part is included in the Asia area,
- ✓ Africa,
- ✓ North America,
- ✓ South America,
- ✓ Asia: also including the European part of Russia and New Guinea,
- ✓ Australia: this area is actually Oceania less New Guinea,
- ✓ Antarctica.

5.1 Known issues or supposed weaknesses

The L1B & L1C GCP GRI weaknesses are mainly related to coverage issues inherited from the Multi-Layer L1B GRI. This occurred because there was no available data to supplement this initial GRI (i.e. Multi-Layer L1B GRI).

The lack of data can mainly be found in the following areas:

- ✓ Greenland & Northern Canada
The coverage of Greenland includes numerous orbits with very strong overlap. All the orbits could not be completed but at least the geographic coverage is ensured. A very careful selection work has been achieved in order to get some points on the rocky parts of the shore. Only images acquired in July and August were selected for that purpose. At other seasons, the landscape is completely snowy; therefore, it is not possible to select images suited to the GRI.
There are also known missing parts over Nunavut and Yukon territories (Northern Canada) for the same reasons as over Greenland.
- ✓ Equatorial area
South American and African equatorial areas, have some gaps in their coverage. This particularly true in South America where it was very difficult to find cloud free images or areas where to find points.

See [PHB-ML-L1B-GRI] for more details.

5.2 Coverage and density

5.2.1 Global coverage

The GRI worldwide geographic coverage obtained is shown on the map of the GCP density in Figure 8.

Please note that the GRI contains all the land-covered areas and includes a long list of small and remote islands.

Here is the almost exhaustive list of remote islands: Iceland, New Zealand, Azores archipelago, Madeira, Canary Islands, Cape Verde, La Réunion, Mauritius, Rodrigues Island, Seychelles, Falkland islands, Galapagos, St Lawrence Island, Hawaiï, Kiribati (partial), Caroline Island, Flint Island, French Polynesia (partial), Samoa, Niué, Neaifu, Tonga, Chatham Island, Pitt Island, Fidji islands, Vanuatu Archipelagos, New Caledonia, Solomon Islands (partial), Svalbard (partial), Commander Island, French Marquesas (partial), Kerguelen, Aleutes (partial), Marianna Island (partial), Clipperton, Pohnpei island, Crozet islands, Socorro island, Admiralty island, Prince Edward islands, Guadalupe.

Figure 8 shows the coverage rate per square degree tile, i.e. the proportion of land covered within a tile considering that a point covers $\sim 50 \text{ km}^2$.

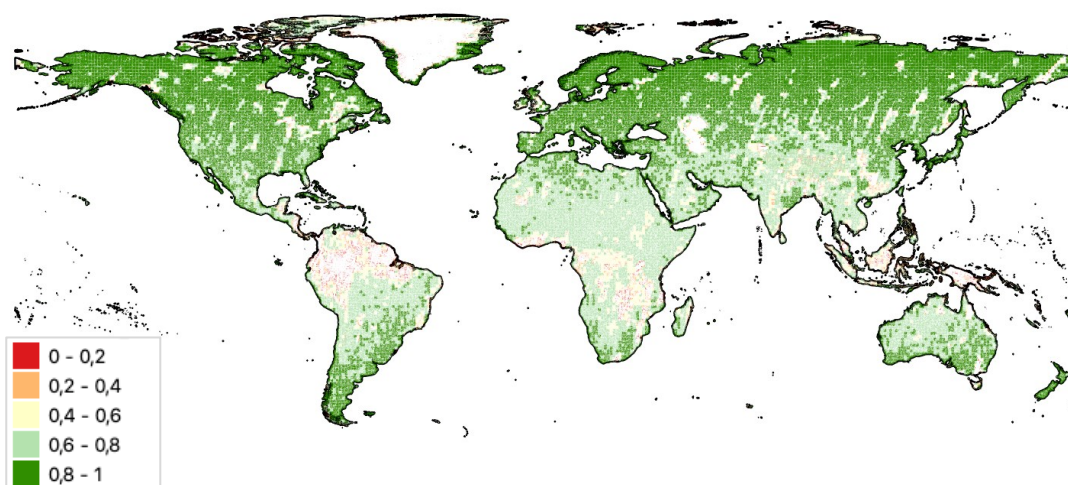


Figure 8: Map of coverage rate of the square degree tiles for the GRI GCP

This map illustrates that the geographic coverage of the L1B & L1C GCP GRI is extensive and well-represented. However, with regards to the numerous constraints (climate, clouds, season, polar night, etc...) and despite a very strong effort, some few areas could not be covered by the Multi-Layer L1B GRI, hence by the L1B & L1C GCP GRI which are built based on the initial GRI (i.e. the Multi-Layer L1B GRI).

Please note that for all the tables and figures presented in this section, all the values **take into account the real land coverage** within a square degree.

Table 4 summarises the values measured regarding the GCPs density. The L1B & L1C GCP GRI are composed of ~ 17900 square degrees.

Table 4: Synthesis of the GCPs final density for the GCP GRI global coverage

Average density	350
tiles with density [200;400]	88,5 %
tiles with density [100;200]	4 %
tiles with density [50;100]	2,9 %
tiles with density [0;50]	4,6 %
tiles visually checked	>1300

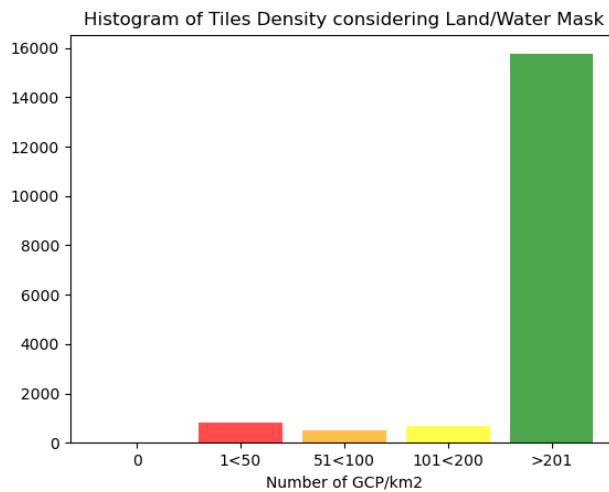


Figure 9: Distribution of the density of the square degrees

Figure 10 shows the GCP density per square degree. Nota, the initial requirement for the density is to have an average of 200 GCPs per square degree.

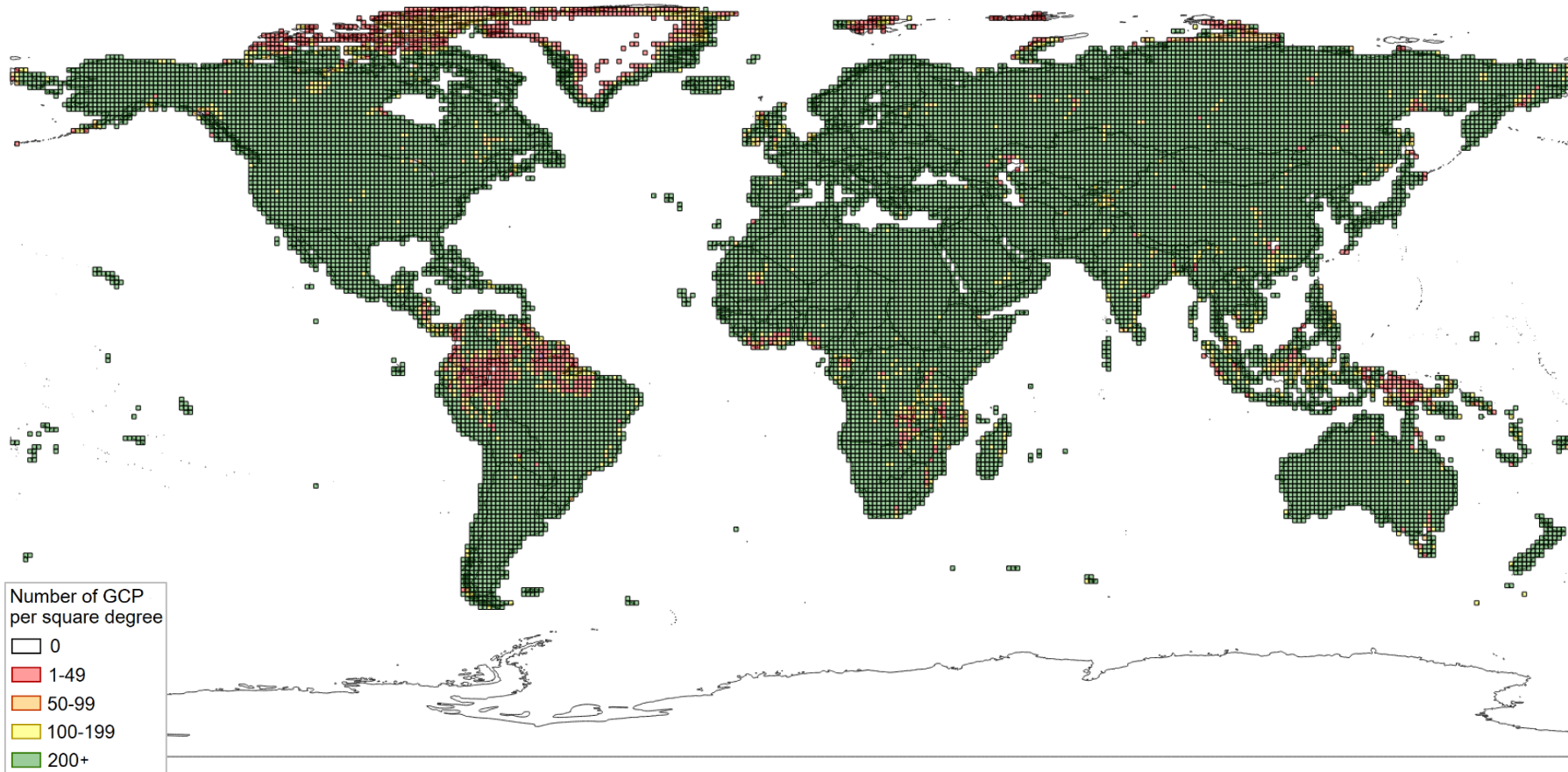


Figure 10: Map of GCPs density per square degree for the GRI GCP

In the following sections details are provided for each area of the world.
 Note that the density is computed taking into account the real land coverage of the square degrees.

5.2.1.1 Europe

We remind that this area doesn't include the European part of Russia that has been considered in Asia block (see section 5.2.1.5).

Figure 11 displays the density of GCP per square degree for Europe, while Figure 12 illustrates the distribution of the GCP density per square degree over the same area.

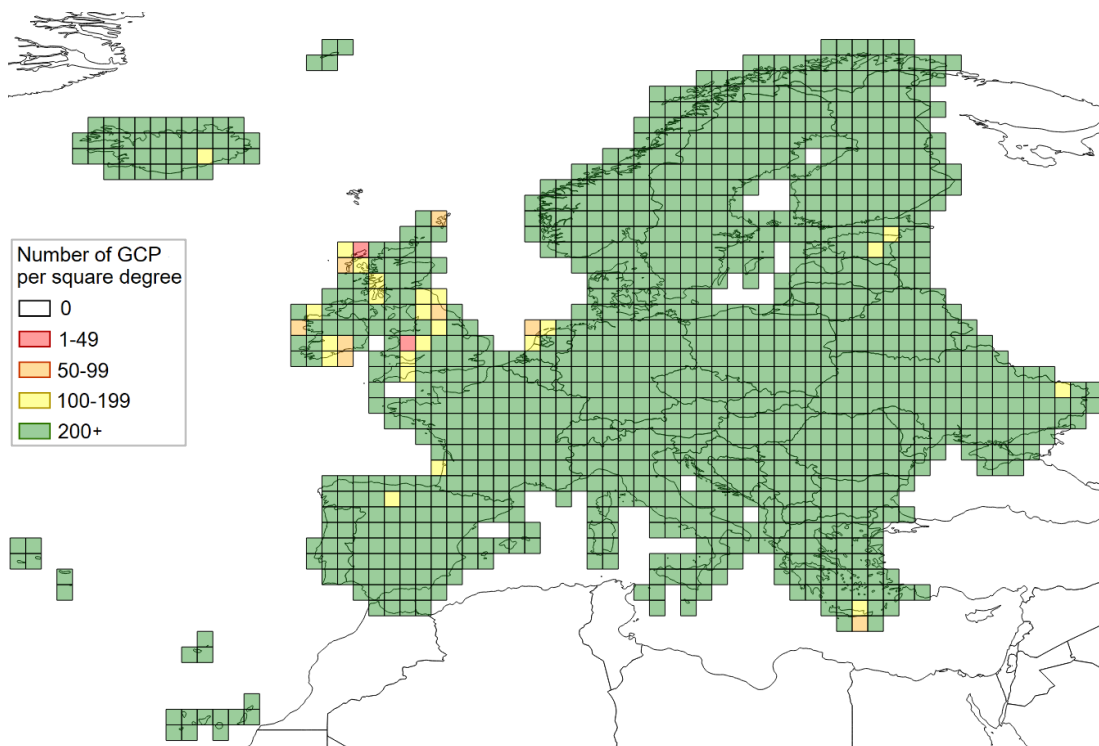


Figure 11: Map of GCP density per square degree for Europe

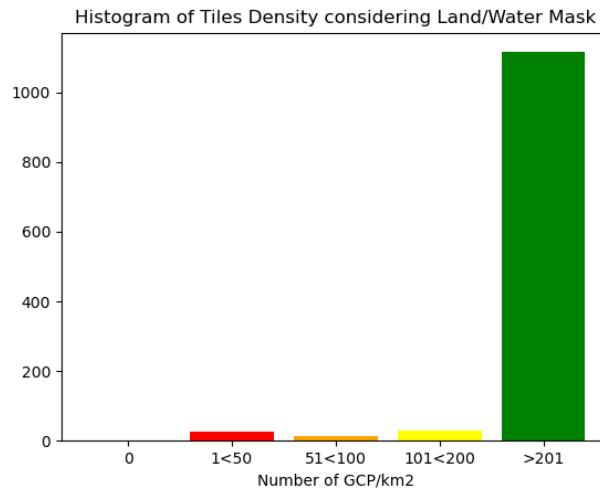


Figure 12: Distribution of the density of the square degrees over Europe

The above density map and histogram show a very good density coverage. Only few square degrees have a density lower than 200 pts, and this is due to the fact that there are over icy or cloudy areas where it was not possible to find images of visible land. This is mainly the case for Svalbard (covered by both ice and clouds) and British Islands (clouds).

5.2.1.2 Africa

Figure 13 shows the density of GCP per square degree for Africa.

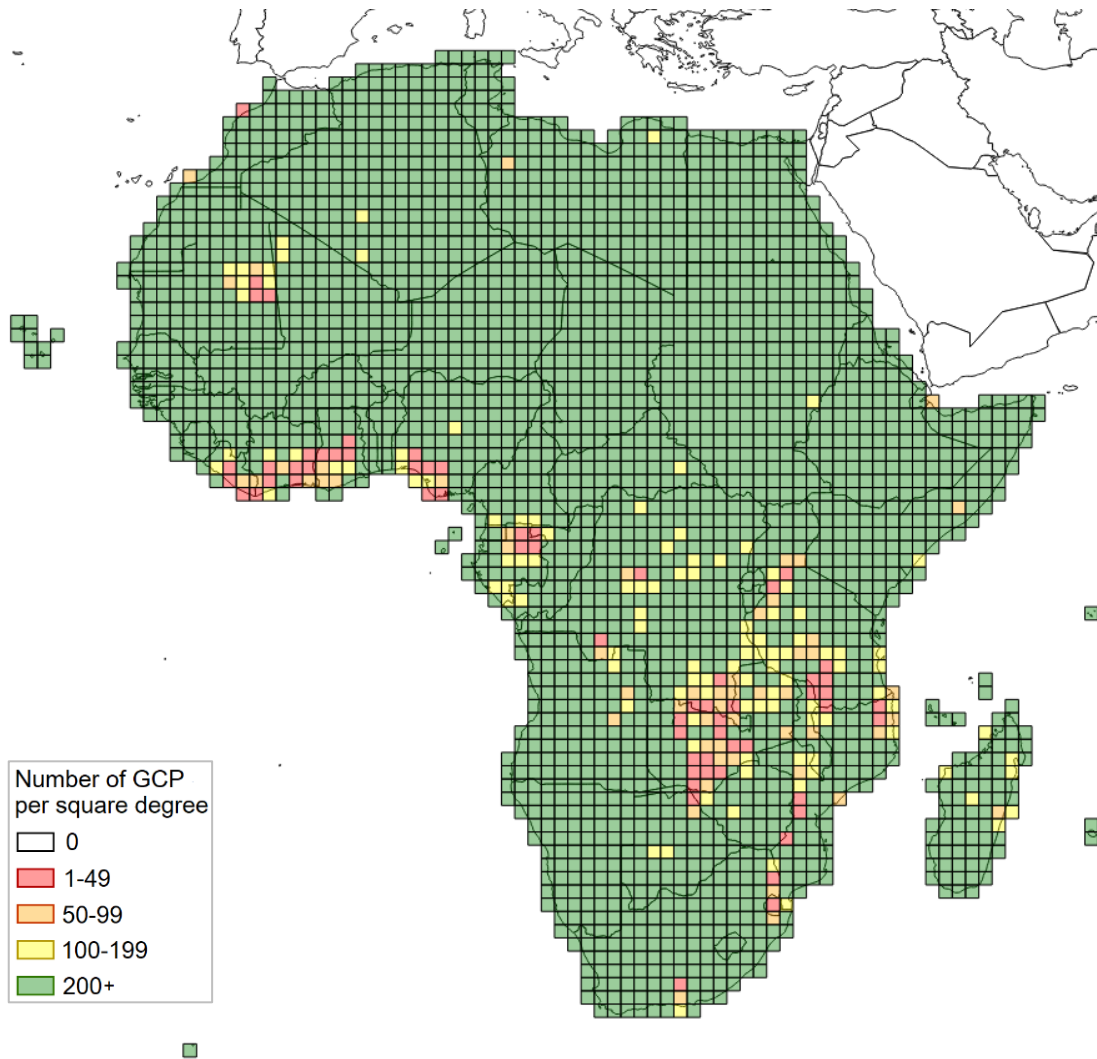


Figure 13: Map of GCP density per square degree for Africa

Figure 14 shows the distribution of the GCP density per square degree for Africa.

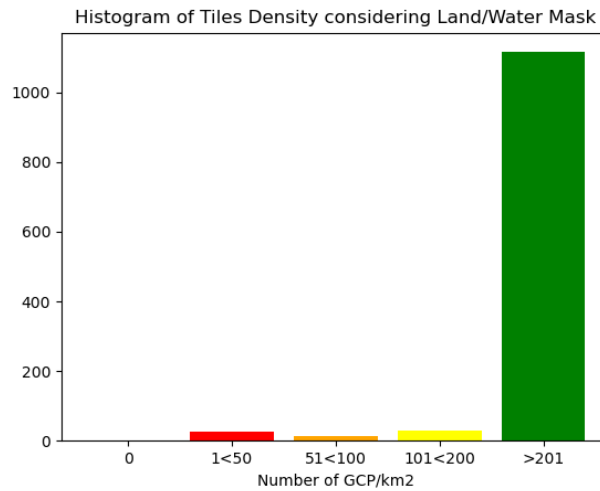


Figure 14: Distribution of the density of the square degrees over Africa

The density map and histogram for Africa reveal that most of the square degrees reach the requirements threshold of 200 points. Only few square degrees fall below this threshold of 200 points because these particular areas are characterized by heavy cloud cover, making it challenging to locate images of visible land.

For more details you can refer to the map of the cloudy pixel percentage per GCP over Africa available in the Validation Report [VAL-L1B-L1C-GCP]. This map highlights the consistency between the cloudy areas and square degrees GCP density below 200 pts.

It can be noted that the land mask used to compute the density of GCP doesn't include the Victoria, Tanganika and Malawi Lakes. Hence the computation doesn't consider water areas to ensure accurate density calculations.

5.2.1.3 North America

Figure 15 shows the density of GCP per square degree for North America.

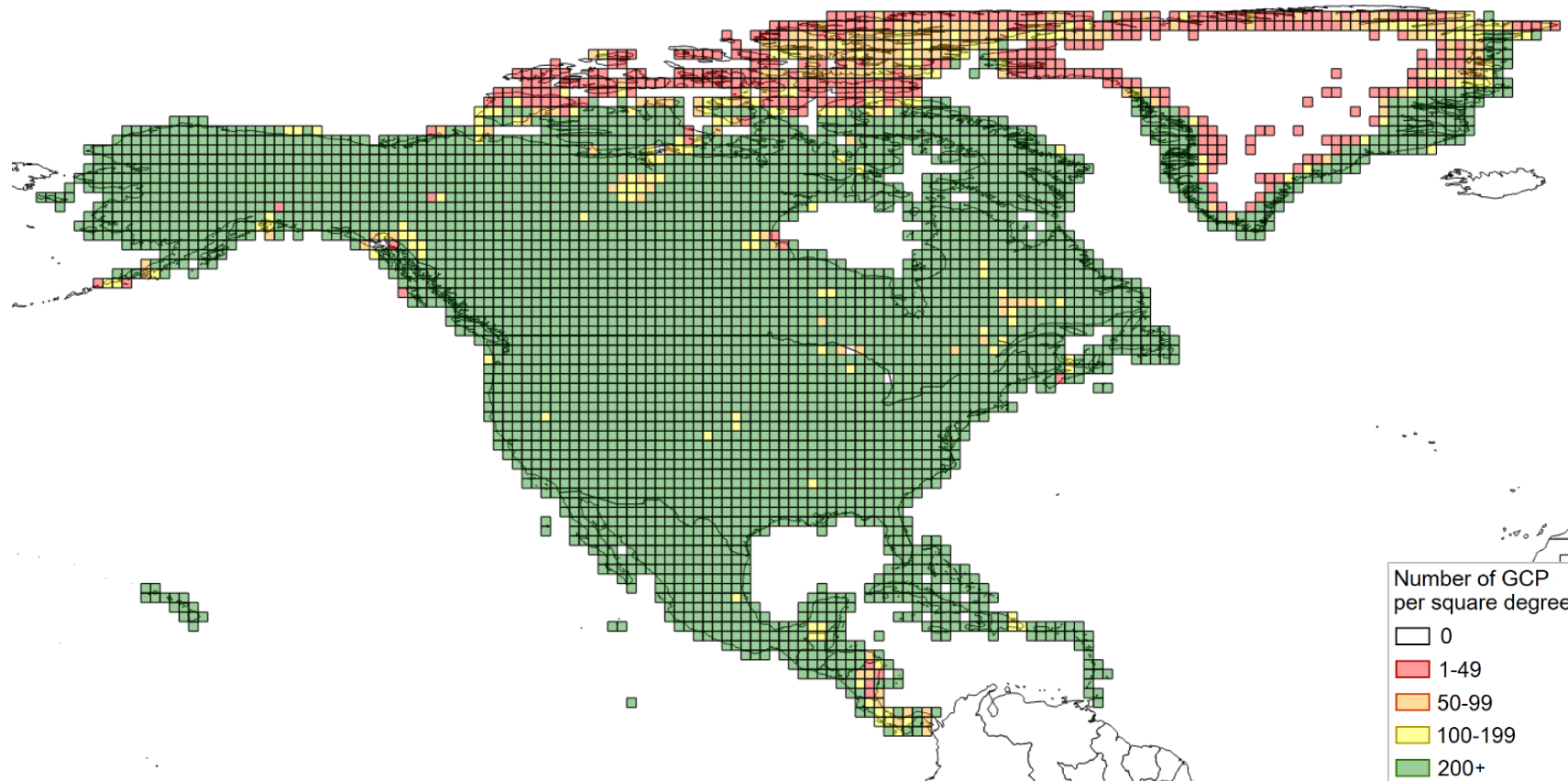


Figure 15: Map of GCP density per square degree for North America

Figure 16 shows the distribution of the GCP density per square degree for North America.

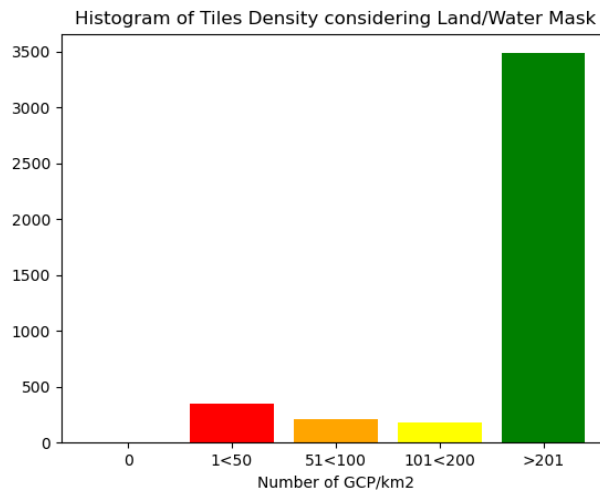


Figure 16: Distribution of the density of the square degrees over North America

The density map and histogram for North America show a very good coverage of North America mainland.

Most of the square degrees with low density are, as expected, over northern latitudes, i.e. Greenland, Nunavut and Yukon Territories, consistently with the original Multi-Layer L1B GRI where it was not possible to find images suited to the GRI.

Some other square degrees not reaching the threshold of 200 pts are also present in mainland, they are mostly due to the presence of the lakes (which are not present in the land mask used for the computation of the density).

5.2.1.4 South America

Figure 17 shows the density of GCP per square degree for South America.

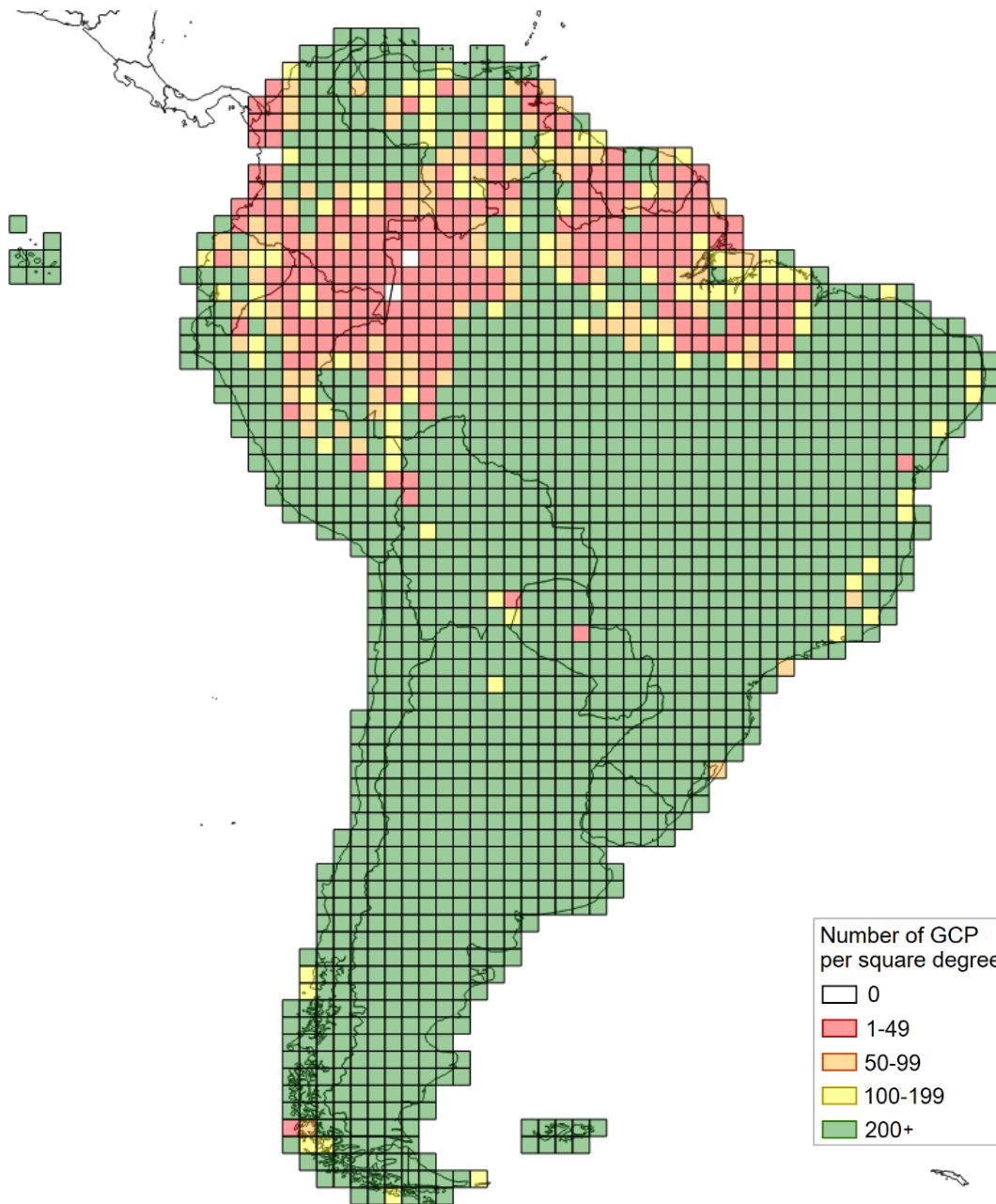


Figure 17: Map of GCP density per square degree for South America

Figure 18 shows the distribution of the GCP density per square degree for South America.

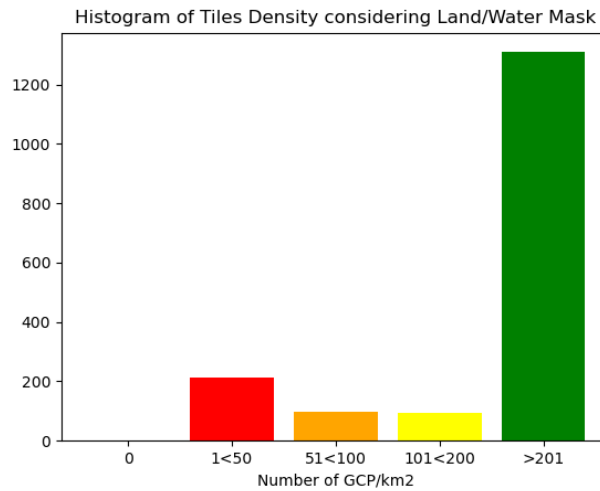


Figure 18: Distribution of the density of the square degrees over South America

The density map and histogram for South America reveal that many of the square degrees reach the requirements threshold of 200 points. Nevertheless, this area also contains a large number of areas with a low GCP density. This is consistent with the known weakness of the Multi-Layer L1B GRI on equatorial areas.

Indeed, even if the Multi-Layer GRI has been built with a strong number of layers on these areas, it was anyway difficult to extract a high number of GCP.

5.2.1.5 Asia

Figure 19 shows the density of GCP per square degree for Asia.

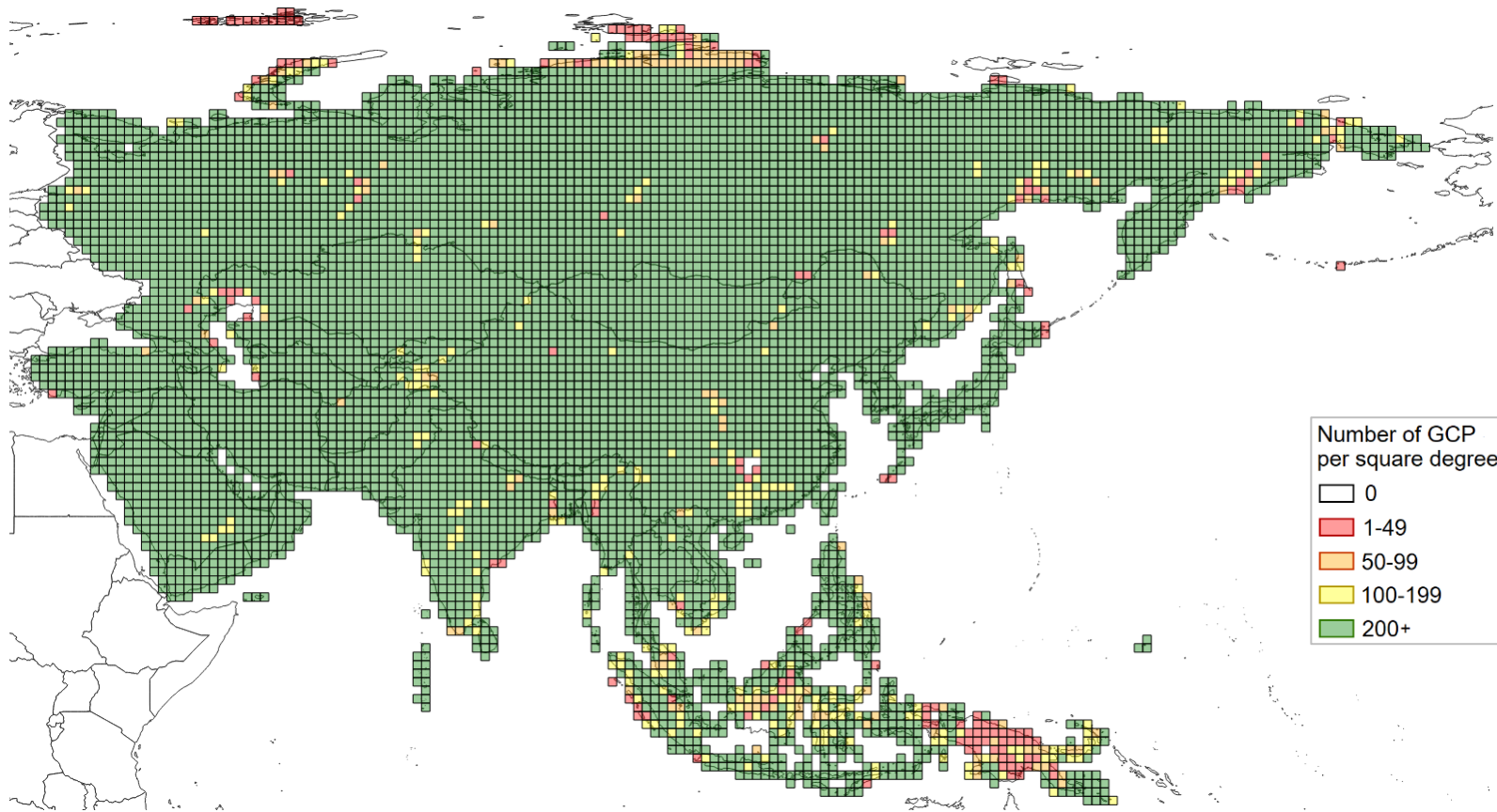


Figure 19: Map of GCP density per square degree for Asia

As shown in the map, we remind that this area also includes the European part of Russia and New Guinea.

Figure 20 shows the distribution of the GCP density per square degree for Asia.

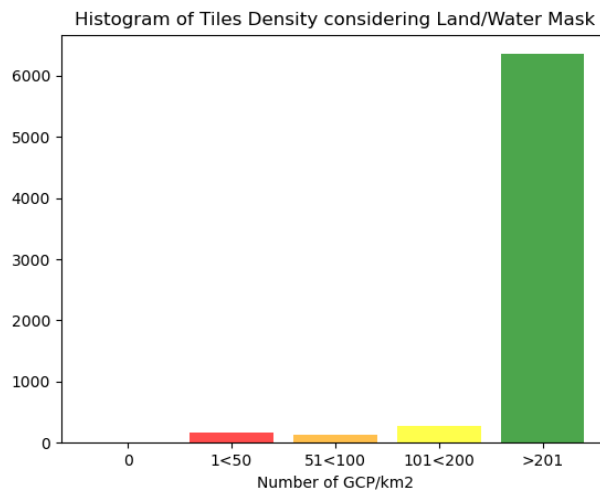


Figure 20: Distribution of the density of the square degrees over Asia

The density map and histogram for Asia reveal that most of the square degrees reach the requirements threshold of 200 points. Only few square degrees fall below this threshold of 200 points. This is consistent with the known weakness of the Multi-Layer L1B GRI.

5.2.1.6 Australia

Figure 21 shows the density of GCP per square degree for Australia.

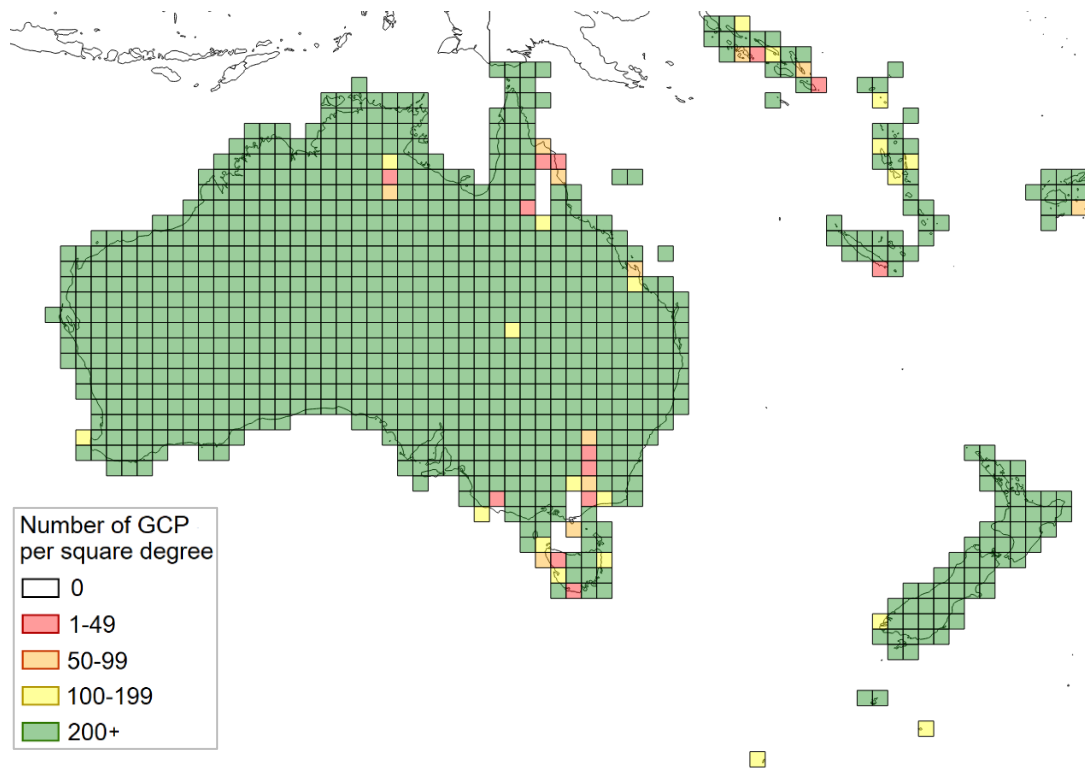


Figure 21: Map of GCP density per square degree for Australia

Figure 22 shows the distribution of the GCP density per square degree for Australia.

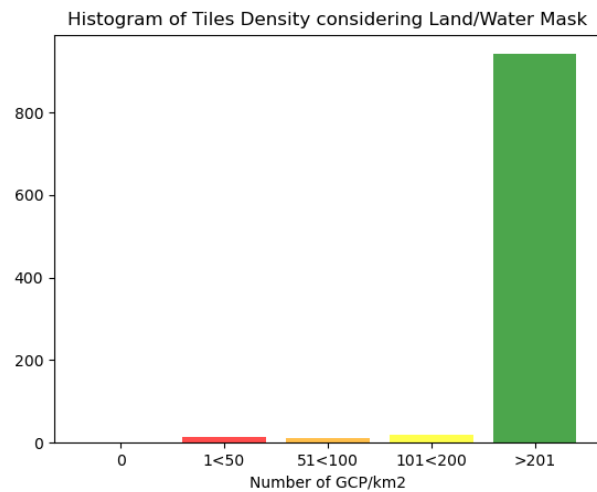


Figure 22: Distribution of the density of the square degrees over Australia

The density map and histogram for Australia show a very good GCP density. The square degrees less covered correspond to very cloudy datastrips in the original Multi-Layer L1B GRI preventing from finding enough GCP to reach the 200 pts threshold for these areas.

5.2.1.7 Antarctica

Figure 23 shows the density of GCP per square degree for Antarctica.

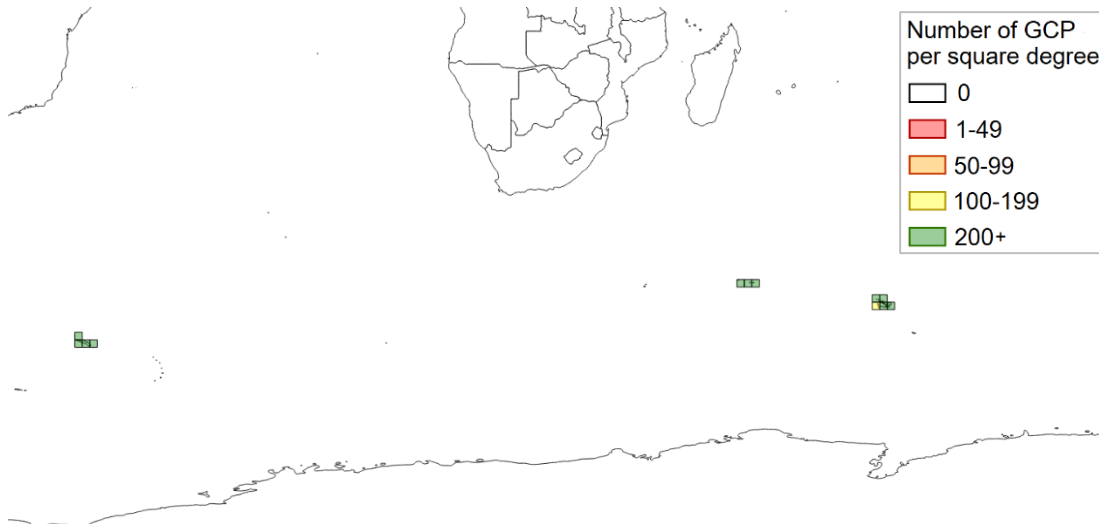


Figure 23: Map of GCP density per square degree for Antarctica

Figure 24 shows the distribution of the GCP density per square degree for Antarctica.

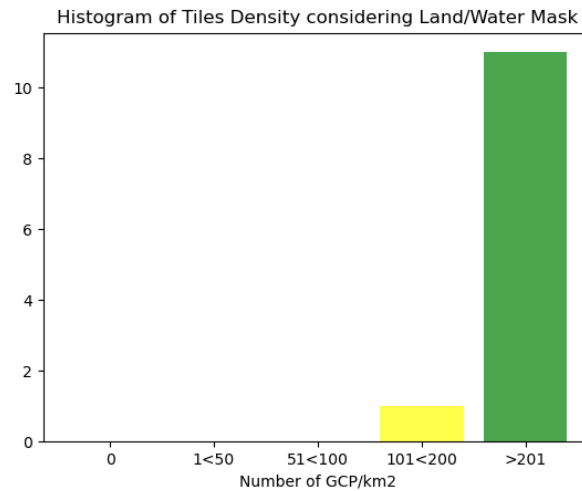


Figure 24: Distribution of the density of the square degrees over Antarctica

There are of course very few GCP over Antarctica, however, the GCP found allow reaching the required density requirement.

5.2.2 Number of chips per GCP

The overlap in the GRI varies according to the areas and depends on the way the Multi-Layer L1B GRI was built. Indeed, an important overlap was planned at continental block intersection, and in general, equatorial areas have also an important overlap so as to reduce the final cloud rate.

This Multi-Layer L1B feature has been inherited by the GCP GRI. The more the Multi-Layer L1B GRI had overlaps, the more the GCP have measures, i.e. overlapped chips.

Furthermore, most of the GCPs selected in the areas where orbits overlap usually have several measures. This is clearly visible in Figure 25.

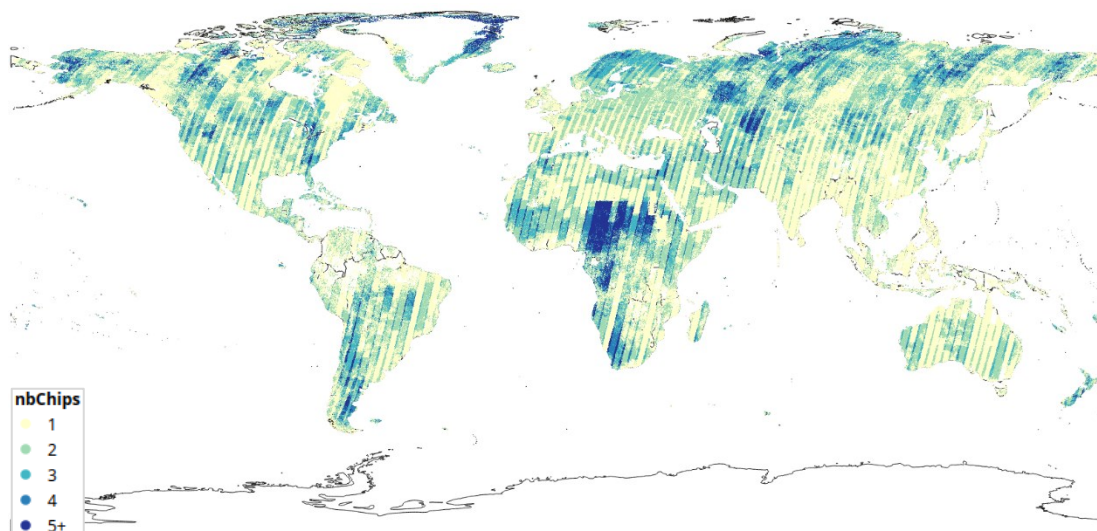


Figure 25: **Number of chips per GCP**

For more information, detailed maps are available in the Validation Report [VAL-L1B-L1C-GCP].

5.3 Geolocation performance

5.3.1 Absolute planimetric accuracy

The geometric accuracy is compliant with Multi-Layer L1B GRI accuracy taking into account Copernicus 30 m DEM accuracy:

- ✓ Absolute geolocation accuracy: 7 m CE95
- ✓ Internal geolocation accuracy: 1 m CE95

5.3.2 Consistency with Multi-Layer L1B & L1C GRI

Details and further results of the validation of the consistency between the L1C GCP GRI and the Multi-Layer L1C (hence L1B) GRI are provided in the Validation Report [VAL-L1B-L1C-GCP].

A summary is provided below.

5.3.2.1 Absolute coherence with Multi-Layer L1C GRI

The Multi-layer L1C GRI and L1C GCP GRI were generated with two different software.

A very good consistency between GCP chips and L1C Tiles coming from the same L1B GRI Datastrip gives good confidence in the projection done for both Multi-Layer and GCP L1C GRI, ensuring that the absolute geolocation of the L1B GRI is well propagated to both L1C GRI.

This is summarized in Figure 26.

The results indicate that the mean distance CE95 is **0.38 m**, which is very good for 10 m resolution images. Please note that the red points in the graph correspond to tiles that have less than 15 chips to correlate with, and therefore, their accuracy cannot be fully guaranteed. As a result, there is strong confidence that the absolute geolocation of L1B GRI is accurately propagated to L1C GCP GRI, meaning **about 7 m**.

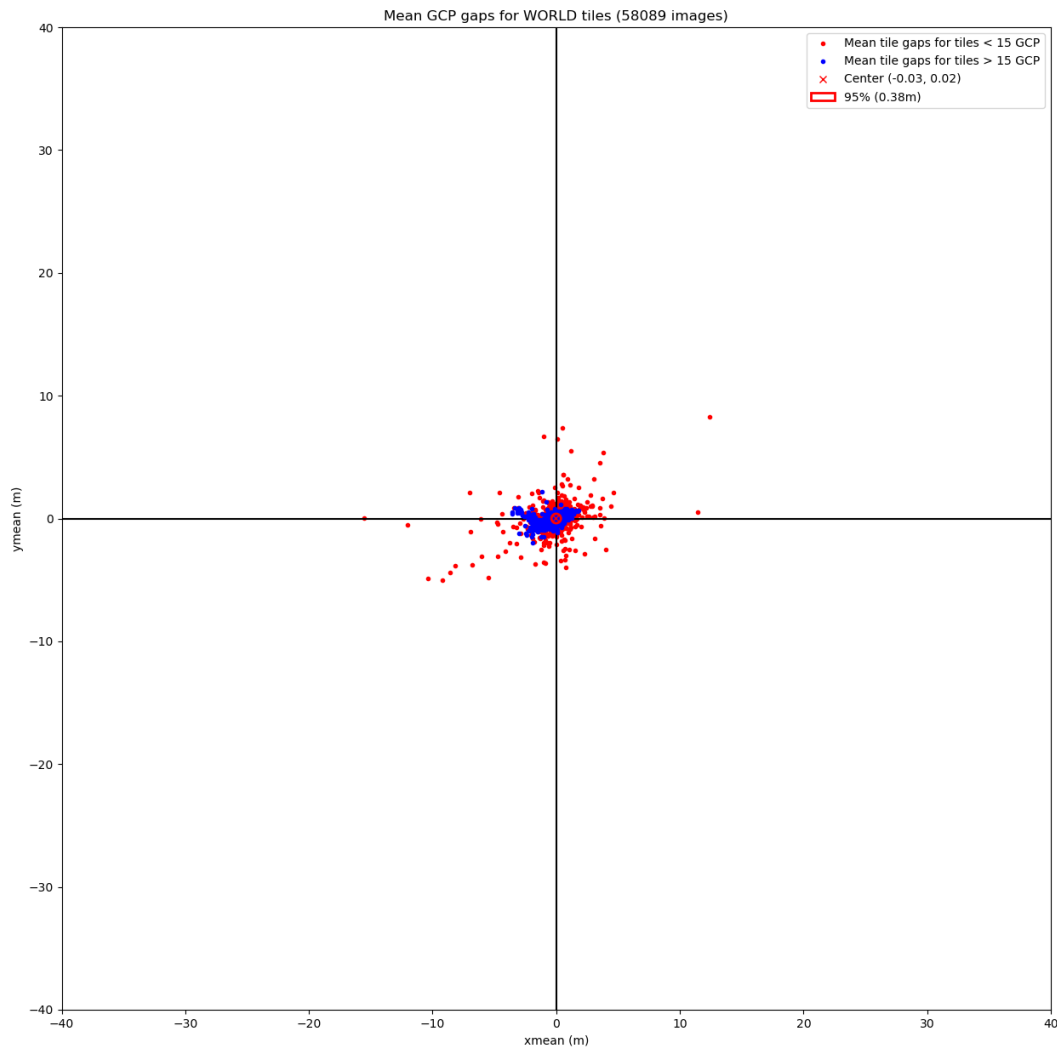


Figure 26: Scatter plot of shifts between L1C Tile and L1C GCP coming from the same L1B datastrip

5.3.2.2 Relative coherence with Multi-Layer L1C GRI

It has been showed in section 5.3.2.1 that a very good consistency (0.60 m) between L1C tiles versus L1C GCPs is obtained. Another exercise was to compare the tiles with chips of GCP that are not extracted from the same datastrip (not to introduce any bias). This gives good results (3.94 m CE95) provided in Figure 27, however this is limited as computed on only tiles with overlapping information.

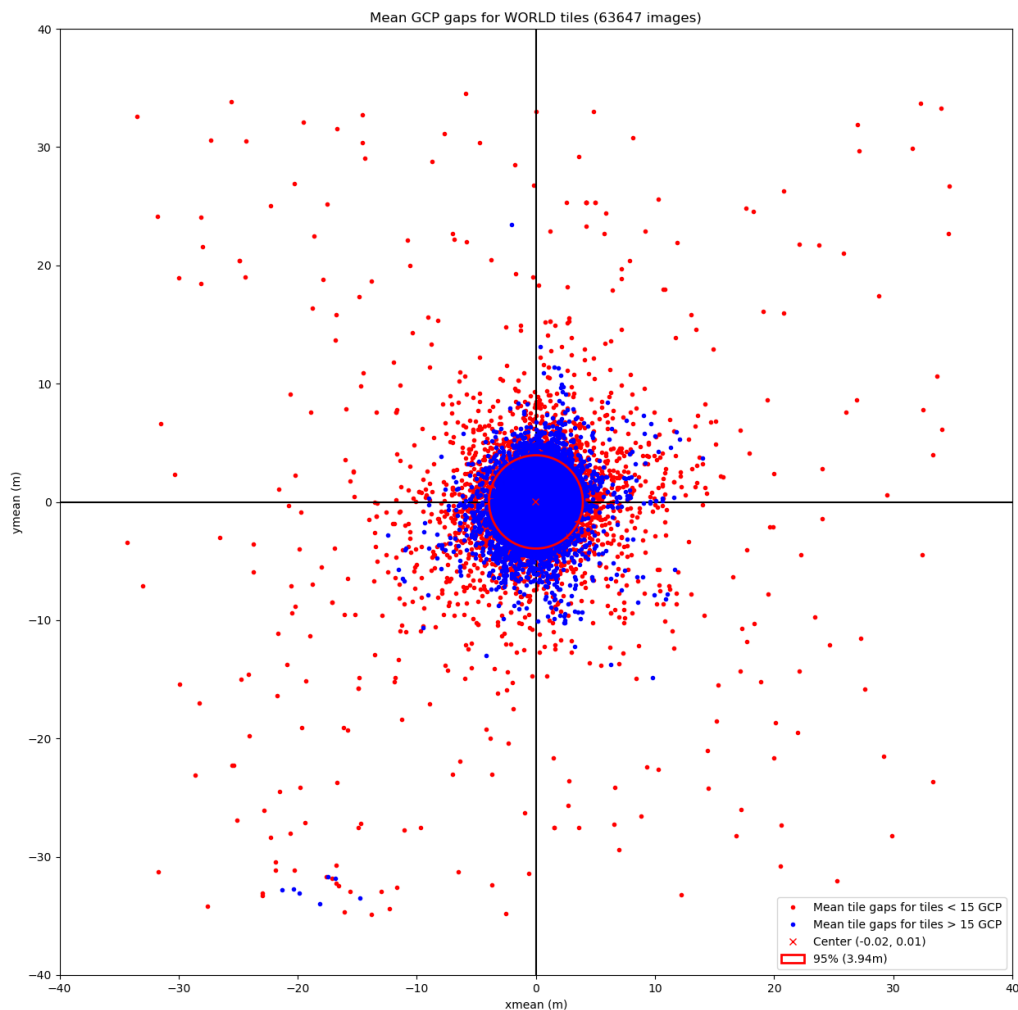


Figure 27: Scatter plot of shifts between L1C Tile and other L1C GCP chips over it (coming from other L1B datastrips)

5.4 GCPs Correlation performance

5.4.1 Seasonal correlation

See section 4.5.4 for details about the computation of the seasonal correlation scores.

It is reminded that two "seasons" have been considered:

1. Summer: from April to September
2. Winter: from October to March

Figure 28 shows the distribution of the GCP according to their seasonal correlation scores for both summer and winter seasons.

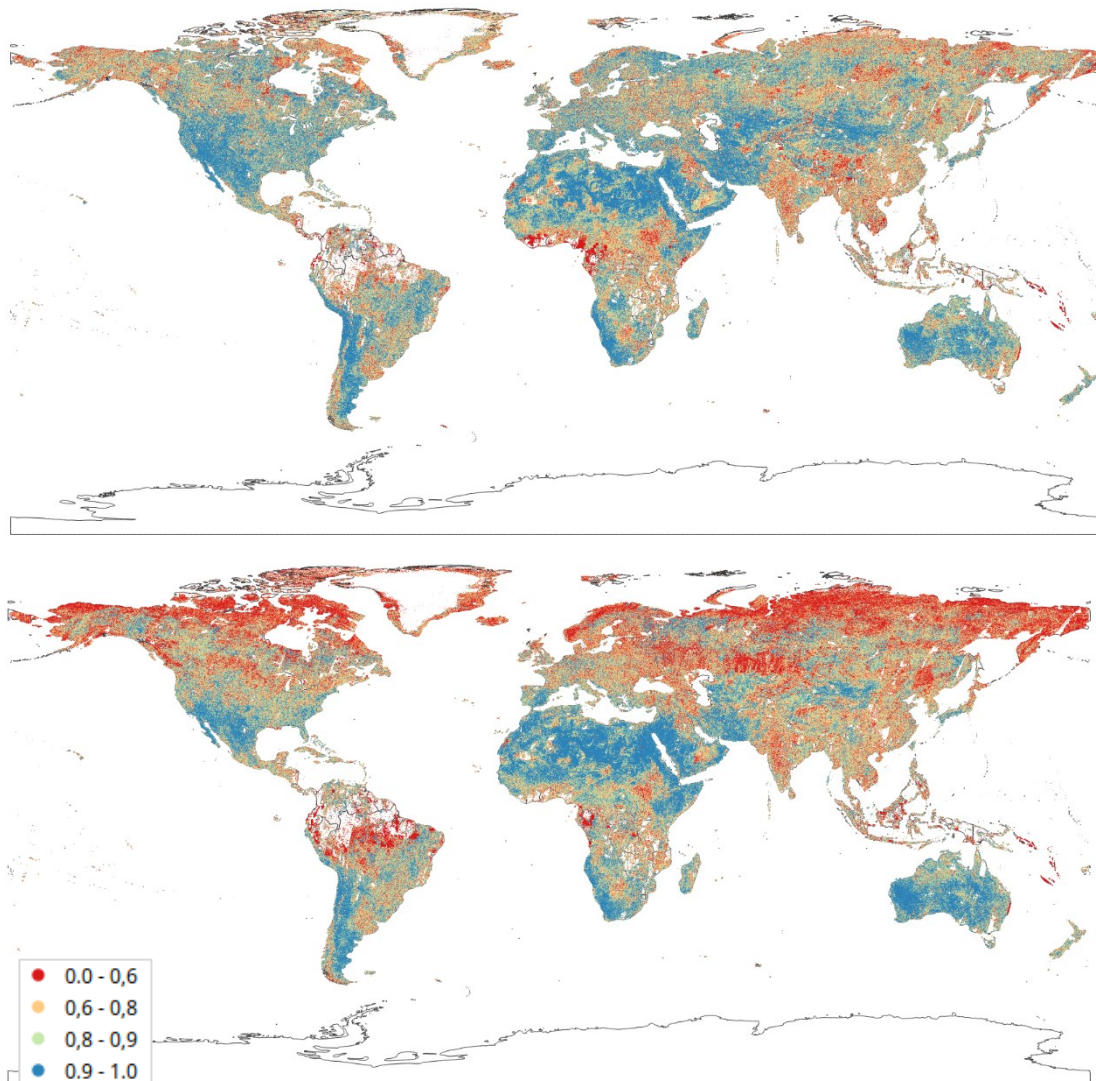


Figure 28: World map of seasonal correlation scores. Top: summer correlation scores. Bottom: winter correlation scores

These maps and particularly the summer one, shows a very good correlation capability for the GCPs.

In winter the red colour highlights areas where the surface is not comparable with the extracted GCP either because the surface has changed since the date of acquisition or due to some seasonal effects.

GCPs in red for both summer and winter correlation assessments highlight areas where the surface has changed since the date of acquisition of the related GRI image.

5.4.1.1 Europe

Figure 29 shows the distribution of the GCP in Europe according to their seasonal correlation scores for both summer and winter seasons.

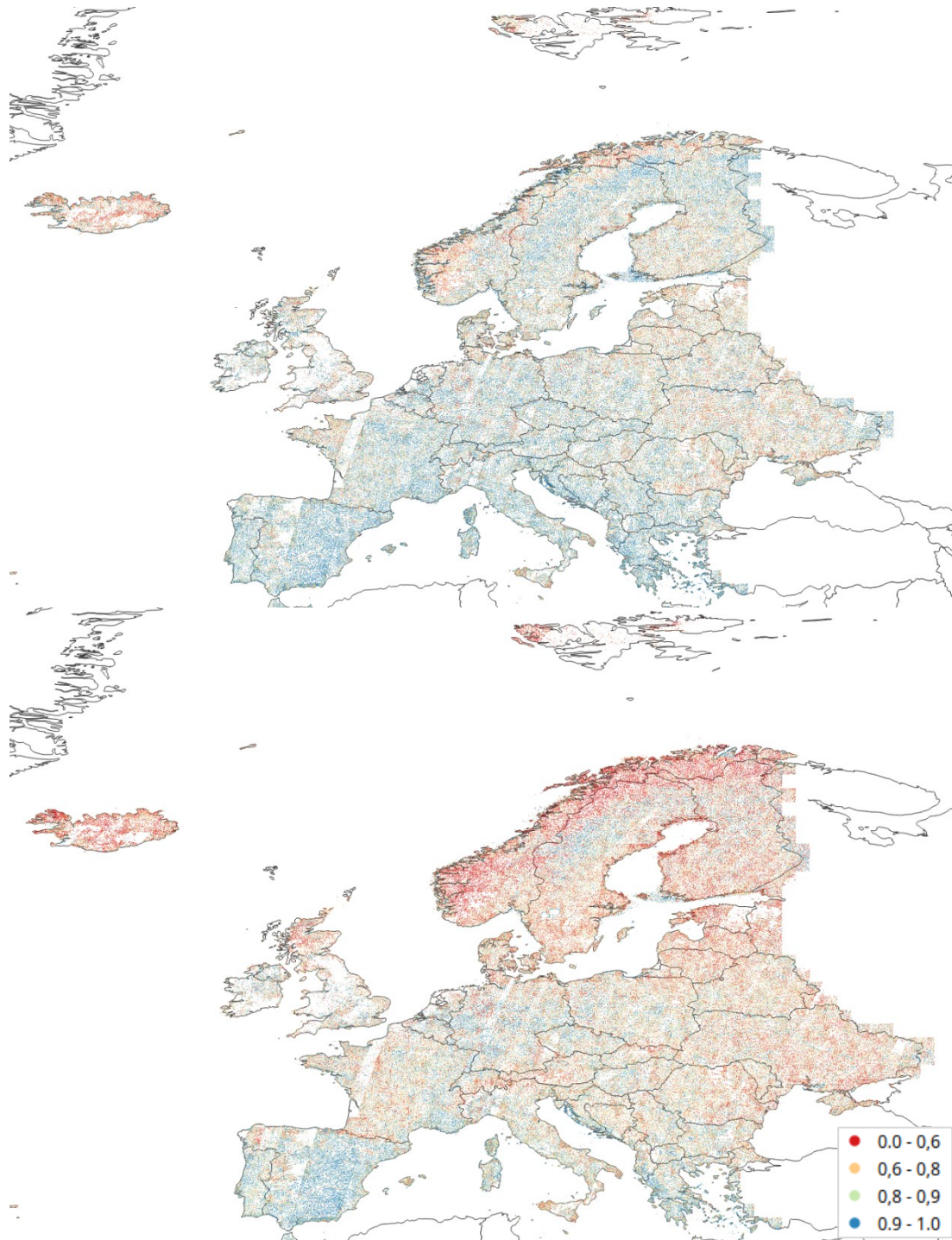


Figure 29: Europe map of seasonal correlation scores. Top: summer correlation scores. Bottom: winter correlation scores

In Europe the correlation scores with recent data remain fairly strong for both seasons.

The seasonal correlation assessment reveals that the correlation of GCPs during wintertime is weaker than during summertime. This discrepancy is particularly noticeable in Norway and Iceland.

However, it is important to notice that in both maps, we can see that there are very good scores (i.e. blue GCP) everywhere, including in Norway even if fewer than in other places.

5.4.1.2 Africa

Figure 30 shows the distribution of the GCP in Africa according to their seasonal correlation scores for both summer and winter seasons.

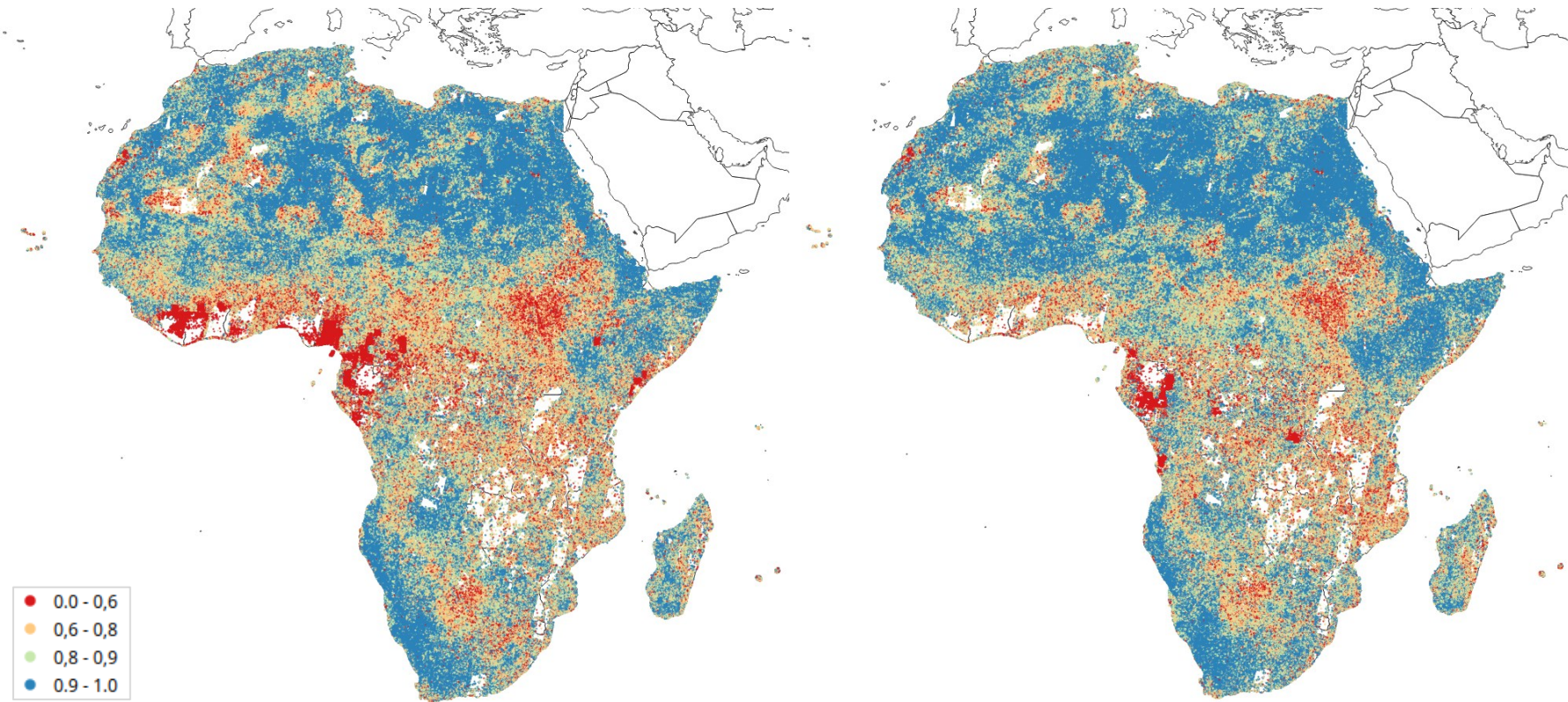


Figure 30: Africa map of seasonal correlation scores. Left: summer correlation scores. Right: winter correlation scores

Based on these maps, we can observe that the correlation scores with recent data remain fairly strong for both seasons. The seasonal correlation assessment reveals that the GCP correlation in Africa doesn't strongly depend on season as both summer and winter maps are quite similar, with slightly better results for the winter season.

The period defined for the summertime exactly matches the rainy season in equatorial area which explains the main differences between the correlation scores for both seasons in this region.

5.4.1.3 North America

Figure 31 shows the distribution of the GCP in North America according to their seasonal correlation scores for both summer and winter seasons.

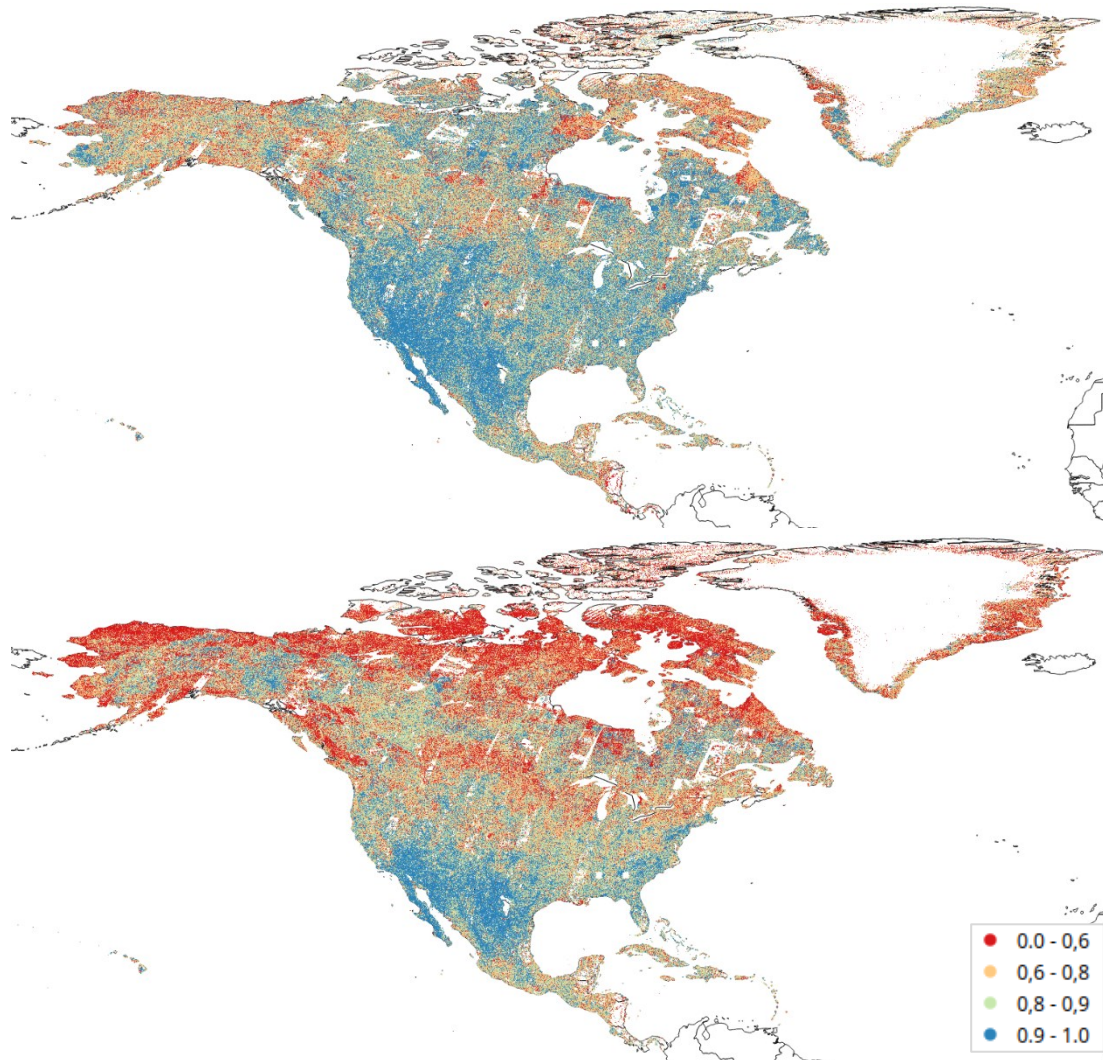


Figure 31: North America map of seasonal correlation scores. Top: summer correlation scores. Bottom: winter correlation scores

The seasonal correlation assessment reveals that the correlation of GCPs during wintertime is weaker compared to summertime, particularly in Northern areas and Greenland.

In Greenland for instance, only images acquired in July and August were chosen to cover the region in the Multi-Layer L1B GRI as during the other seasons the landscape is predominantly covered by snow, making it challenging to select suitable images for the GRI.

5.4.1.4 South America

Figure 32 shows the distribution of the GCP in South America according to their seasonal correlation scores for both summer and winter seasons.

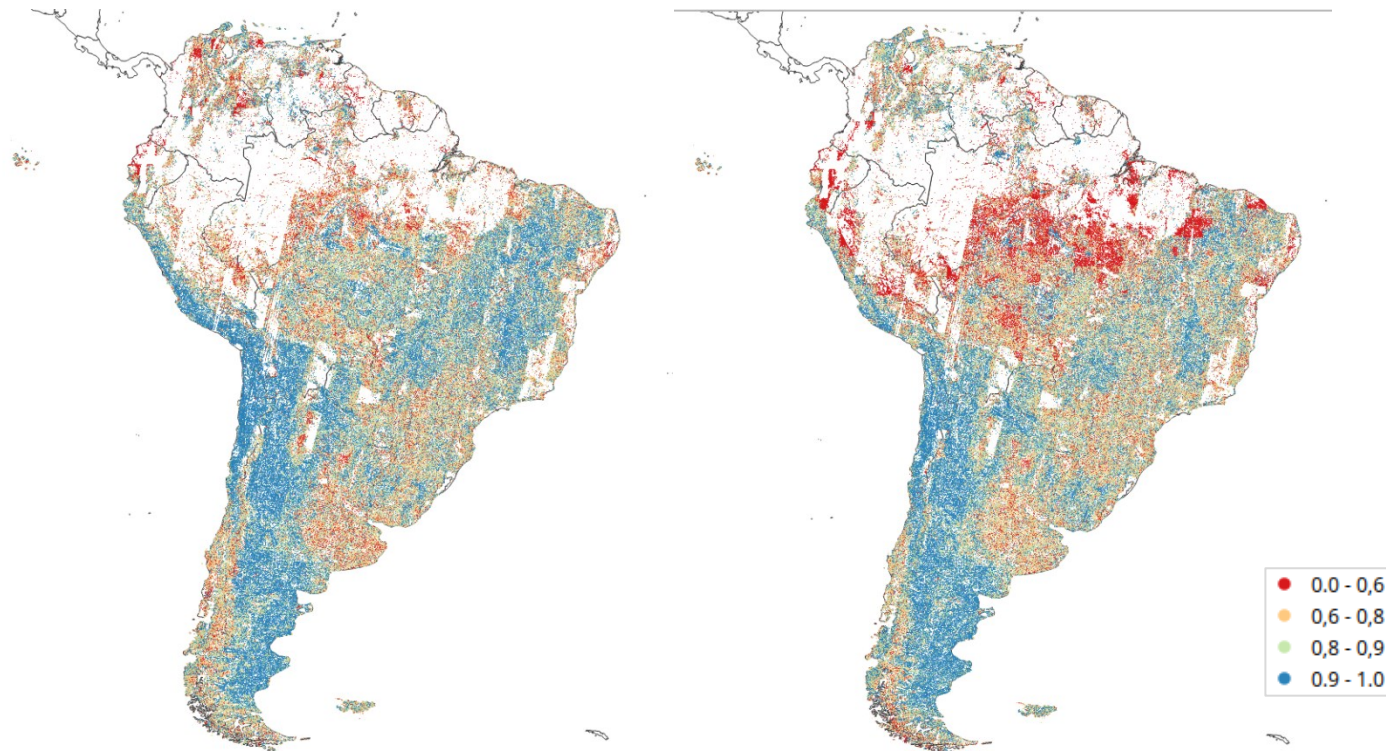


Figure 32: South America map of seasonal correlation scores. Left: summer correlation scores. Right: winter correlation scores

Based on these maps, we can observe that the correlation scores with recent data remain fairly strong for both seasons. The seasonal correlation assessment highlights that the GCP correlation does not show a strong dependency on the season as both summer and winter maps are quite similar, with a slight improvement observed during the Summer season.

5.4.1.5 Asia

Figure 33 shows the distribution of the GCP in Asia according to their seasonal correlation scores for both summer and winter seasons.

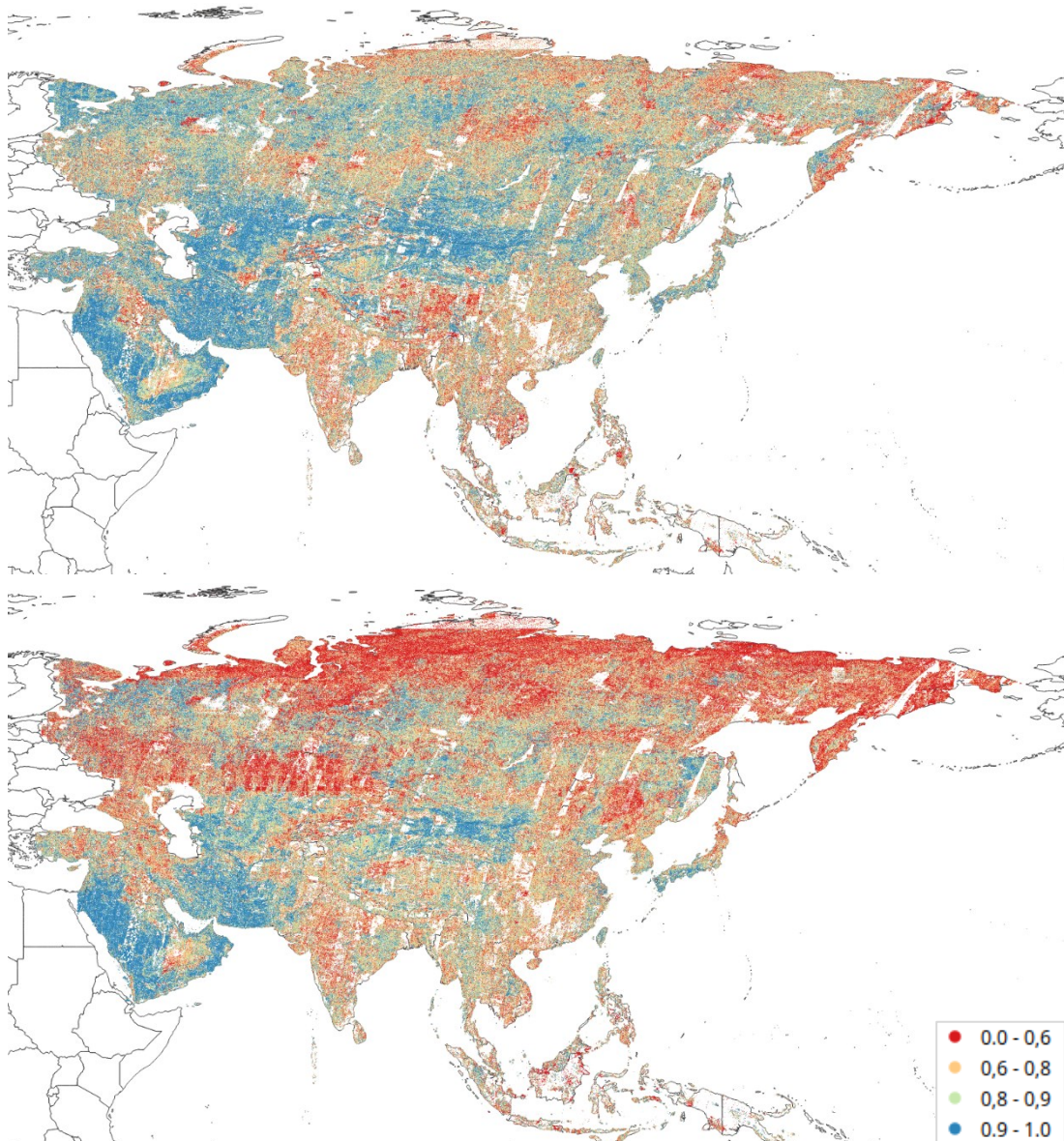


Figure 33: Asia map of seasonal correlation scores. Top: summer correlation scores. Bottom: winter correlation scores

The seasonal correlation assessment reveals that the correlation of GCPs during wintertime is weaker than during summertime. This discrepancy is particularly noticeable in Northern areas.

5.4.1.6 Australia

Figure 34 shows the distribution of the GCP in Australia according to their seasonal correlation scores for both summer and winter seasons.



Figure 34: Australia map of seasonal correlation scores. Top: summer correlation scores. Bottom: winter correlation scores

Based on these maps, we can observe that the correlation scores with recent data remain fairly strong for both seasons.

The seasonal correlation assessment highlights that the GCP correlation does not show a strong dependency on the season as both summer and winter maps are very similar.

5.4.1.7 Antarctica

Figure 35 shows the distribution of the GCP in Antarctica according to their seasonal correlation scores for both summer and winter seasons.

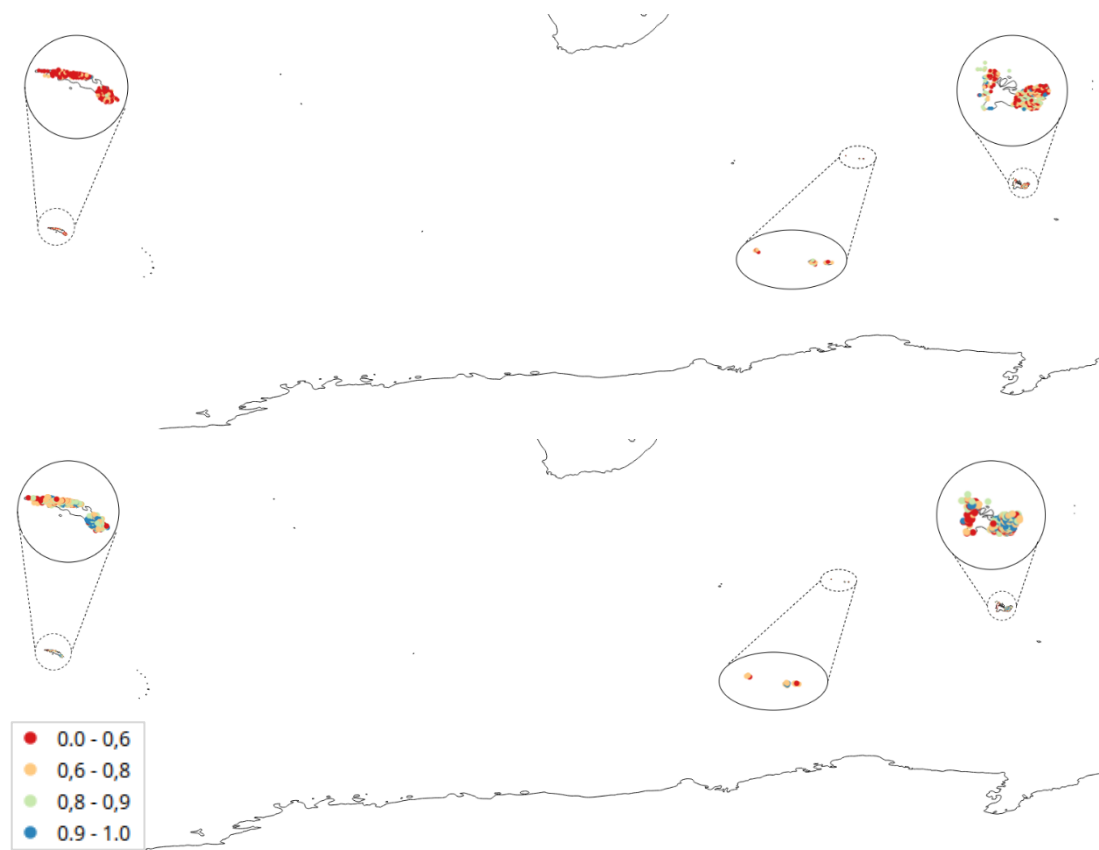


Figure 35: Antarctica map of seasonal correlation scores. Top: summer correlation scores. Bottom: winter correlation scores

Based on these maps, the correlation scores are higher for the winter season compared to the summer season. However, as only a few points are analysed, no final conclusion can be drawn from these maps.

5.4.2 Final Score

The final score is a combination of the correlation and curvature scores, providing an overall assessment of the quality of the GCPs. Indeed, these scores are commonly used to evaluate the quality and accuracy of the data. A trade off was made in the final score definition as both the correlation and curvature scores are

considered by the L1 Sentinel-2 processor for the refining using the Multi-Layer L1B GRI. Final scores are between 1 and 5, 1 being better than 5. For more details about the final score definition please refer to section 4.5.6.

Please note that the curvature scores and anisotropy values are presented in the Validation Report [VAL-L1B-L1C-GCP].

Figure 36 shows the distribution of the GCP in the Word according to their final score.

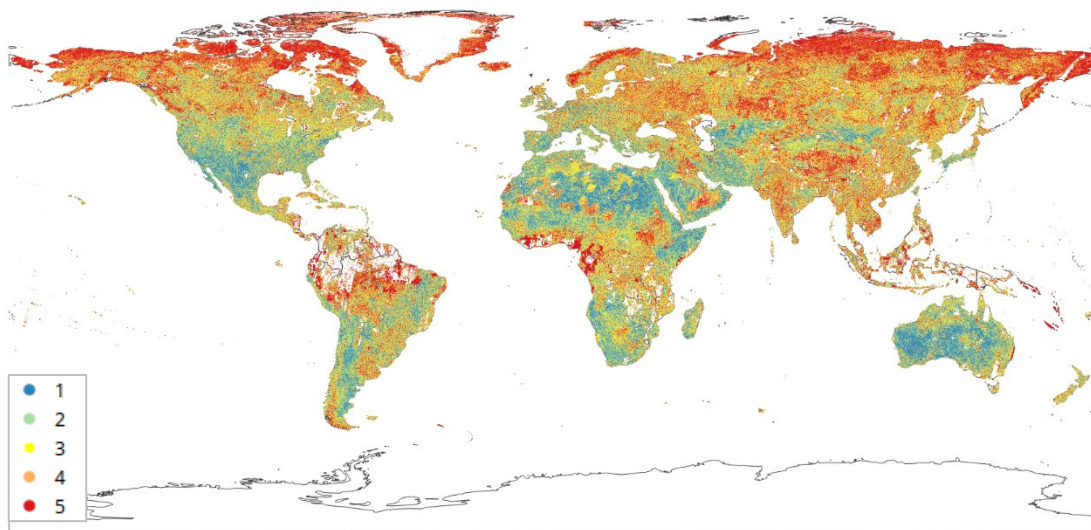


Figure 36: World map of the GCP final scores

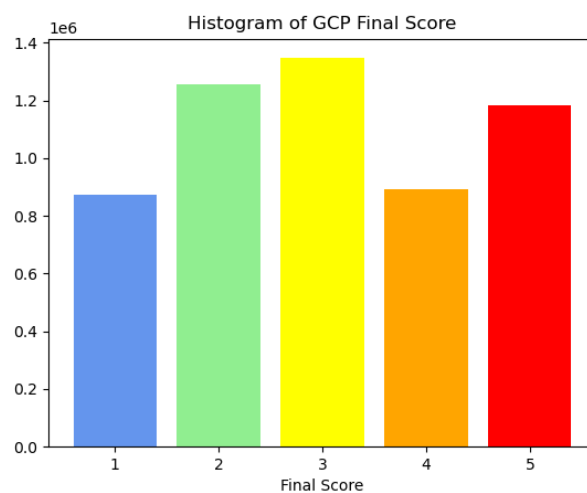


Figure 37: Distribution of the final scores of the GCP

It can be noticed that good final scores are well distributed over the entire world. The zones with a less good final score (e.g. 5) are mostly related to areas where the surface is not comparable with the extracted GCP either because the surface has changed since the date of acquisition or due to some seasonal effects or high cloud cover.

5.4.2.1 Europe

Figure 38 shows the distribution of the GCP in Europe according to their final score.

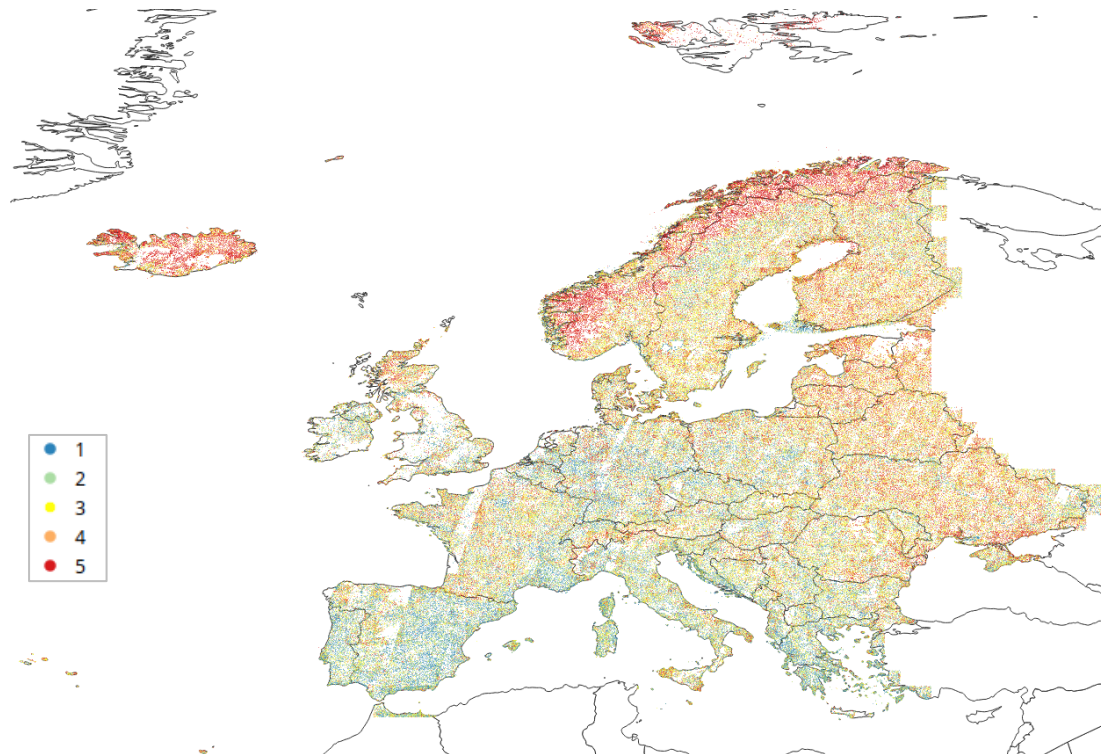


Figure 38: Europe map of the GCP final scores

Figure 39 shows the distribution of the GCP final scores for Europe.

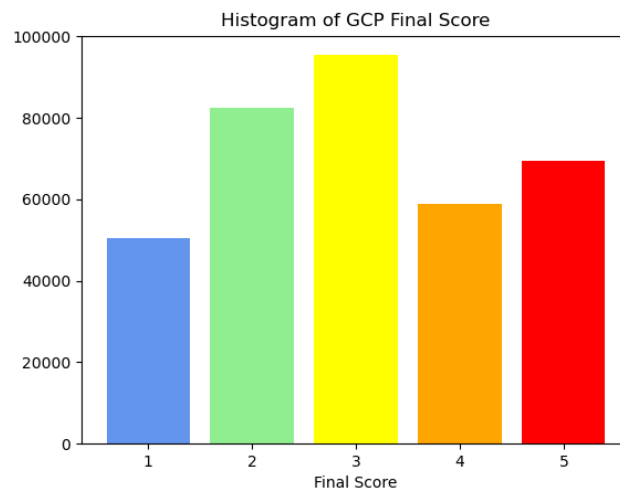


Figure 39: Distribution of the final scores of the GCP over Europe

5.4.2.2 Africa

Figure 40 shows the distribution of the GCP in Africa according to their final score.

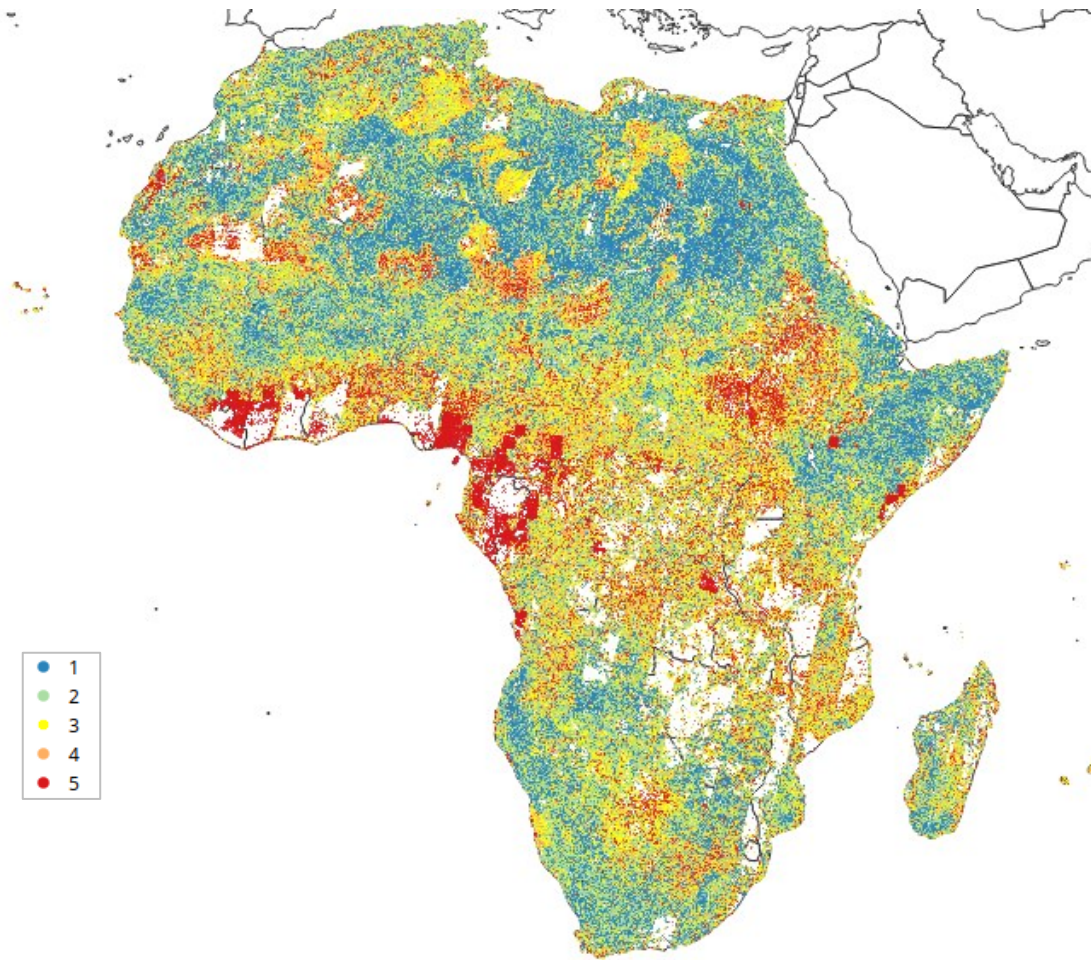


Figure 40: Africa map of the GCP final scores

Figure 41 shows the distribution of the GCP final scores for Africa.

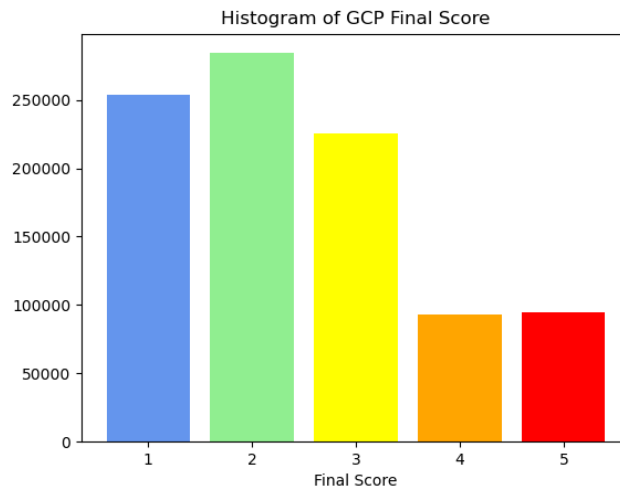


Figure 41: Distribution of the final scores of the GCP over Africa

5.4.2.3 North America

Figure 42 shows the distribution of the GCP in North America according to their final score.

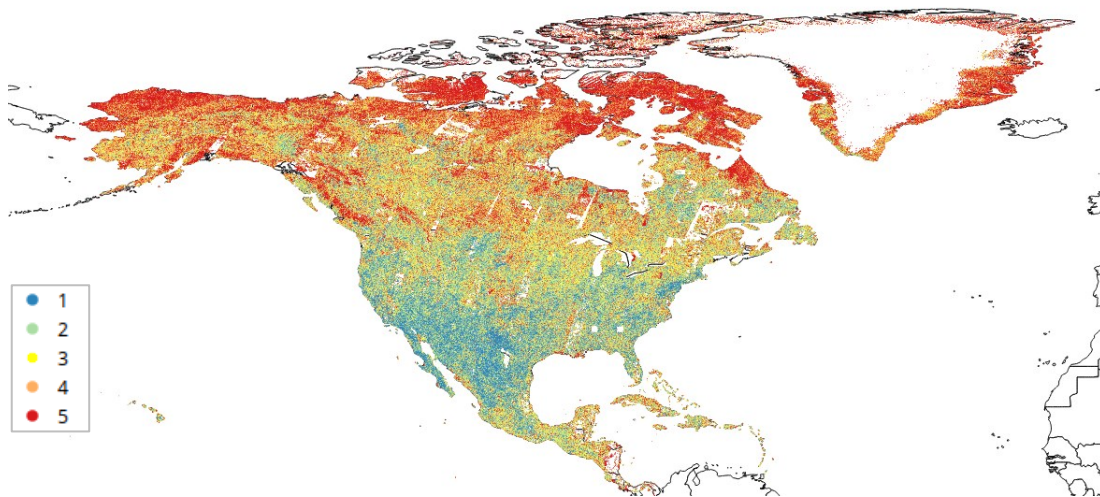


Figure 42: North America map of the GCP final scores

Figure 43 shows the distribution of the GCP final scores for North America.

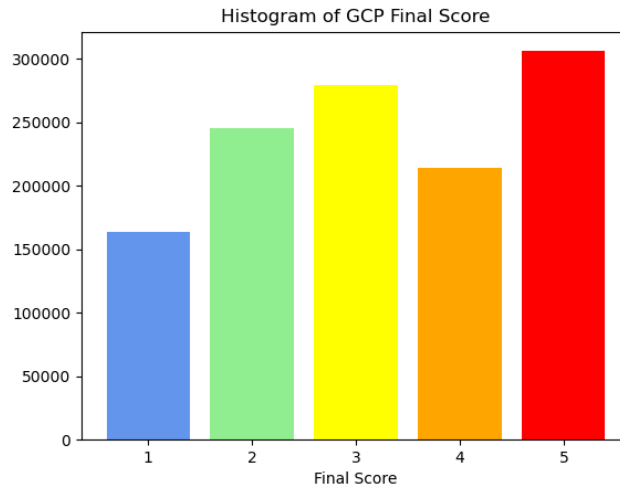


Figure 43: Distribution of the final scores of the GCP over North America

5.4.2.4 South America

Figure 44 shows the distribution of the GCP in South America according to their final score.

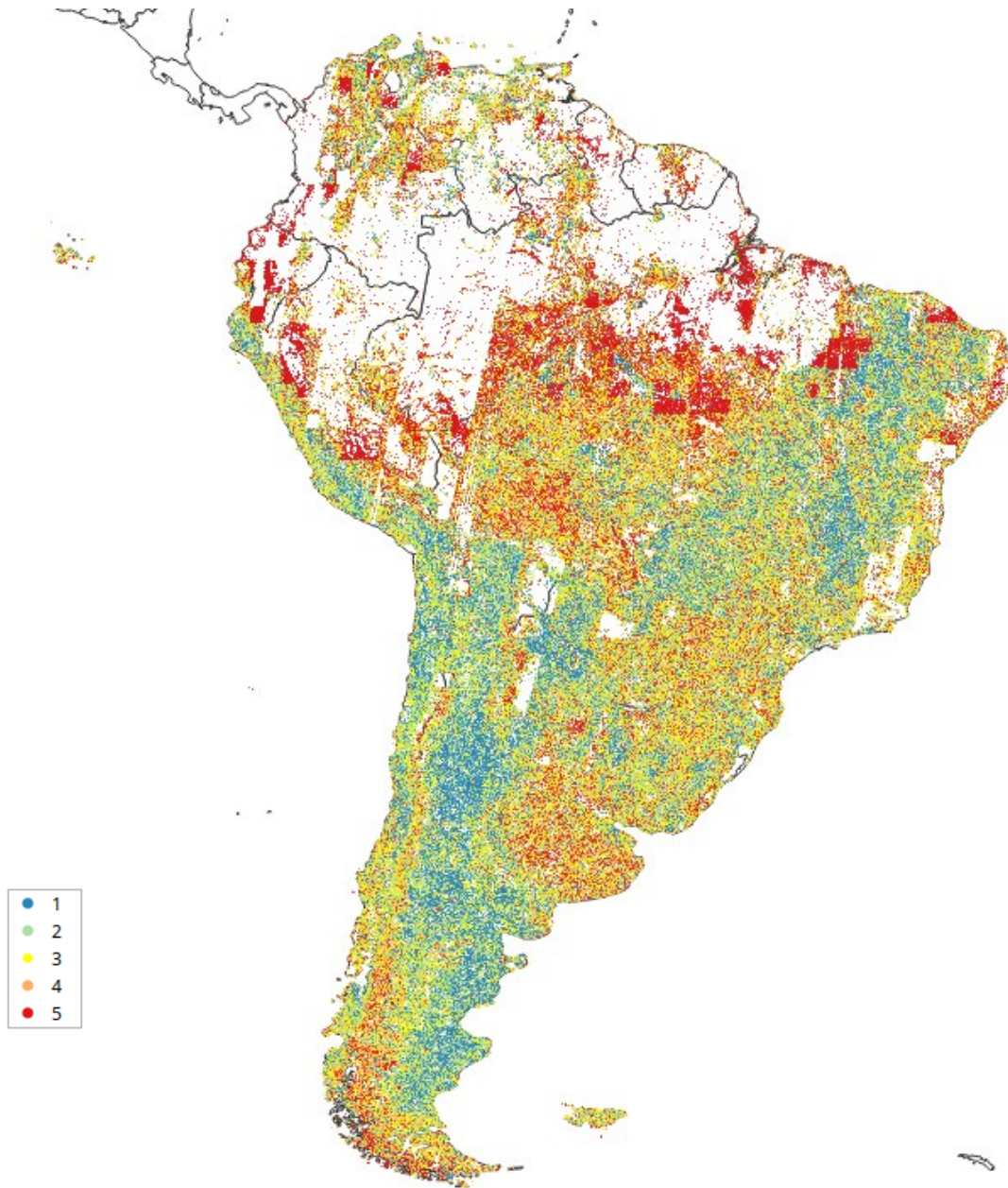


Figure 44: South America map of the GCP final scores

Figure 45 shows the distribution of the GCP final scores for South America.

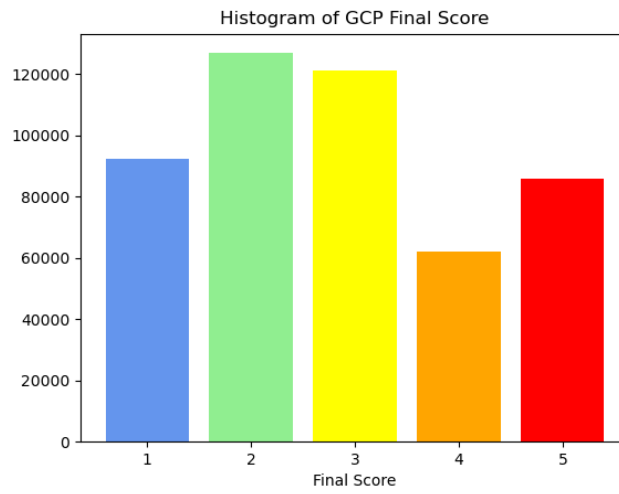


Figure 45: Distribution of the final scores of the GCP over South America

5.4.2.5 [Asia](#)

Figure 46 shows the distribution of the GCP in Asia according to their final score.

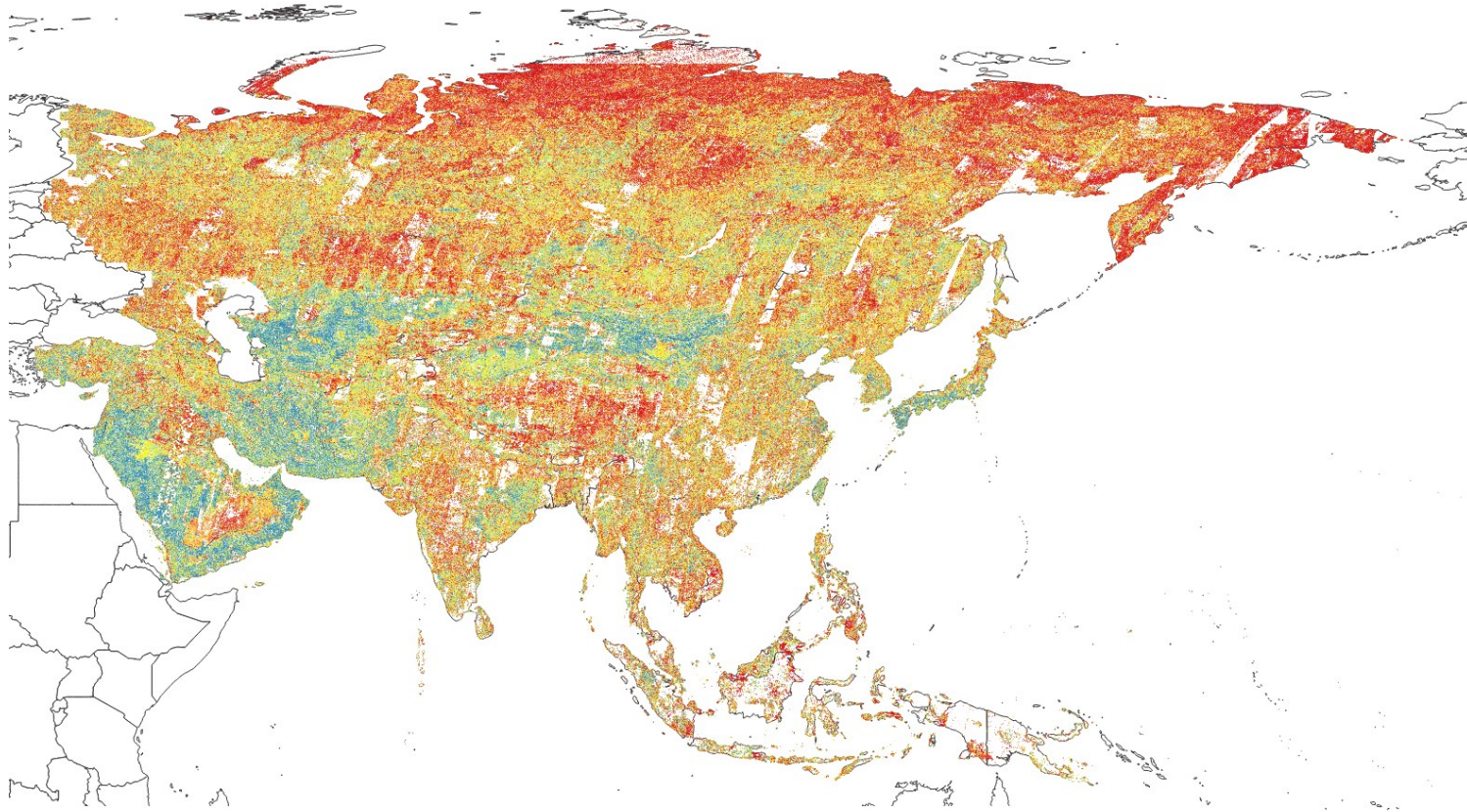


Figure 46: Asia map of the GCP final scores

Figure 47 shows the distribution of the GCP final scores for Asia.

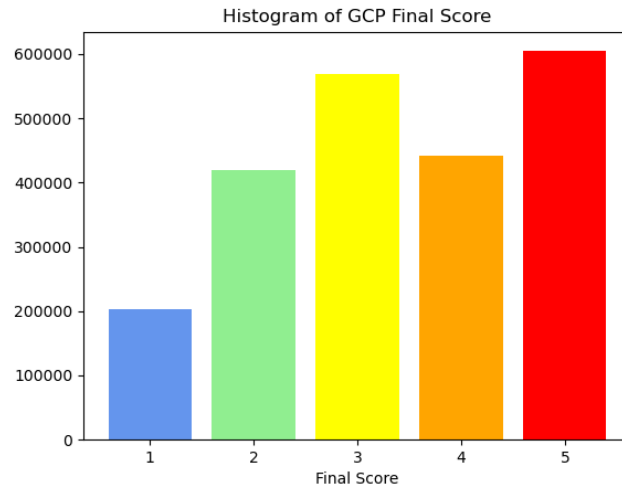


Figure 47: Distribution of the final scores of the GCP over Asia

5.4.2.6 Australia

Figure 48 shows the distribution of the GCP in Australia according to their final score.

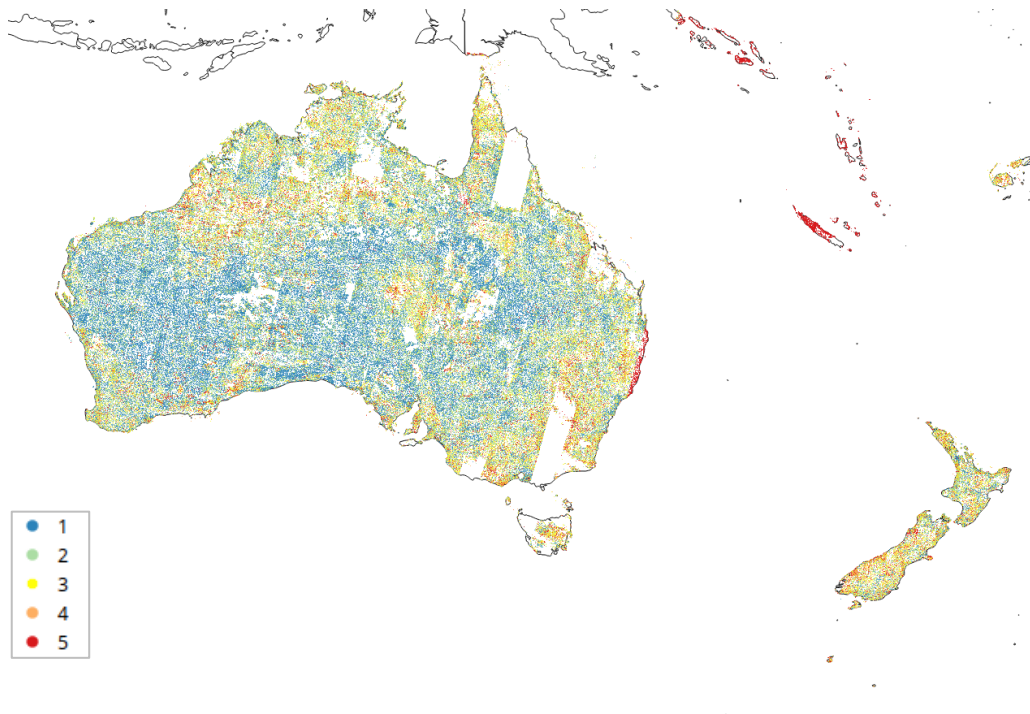


Figure 48: Australia map of the GCP final scores

Figure 49 shows the distribution of the GCP final scores for Australia.

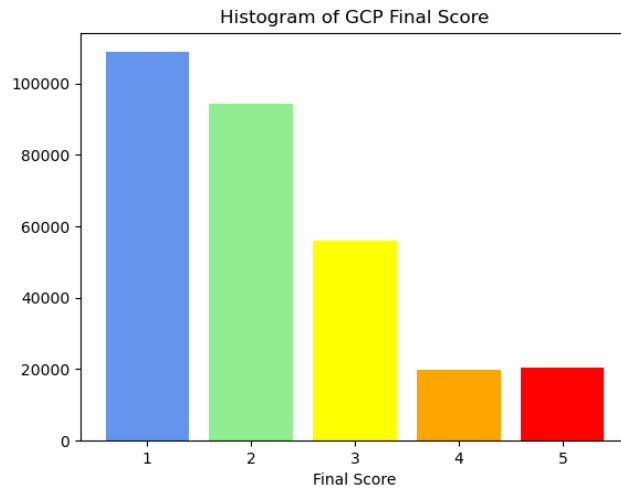


Figure 49: Distribution of the final scores of the GCP over Australia

5.4.2.7 Antarctica

Figure 50 shows the distribution of the GCP in Antarctica according to their final score.



Figure 50: Antarctica map of the GCP final scores

Figure 51 shows the distribution of the GCP final scores for Antarctica.

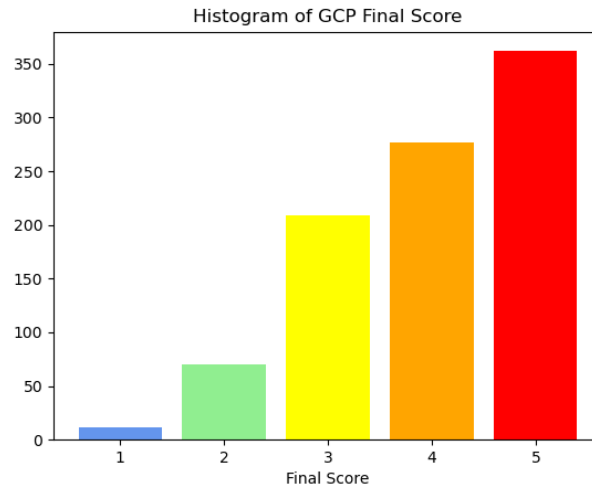


Figure 51: Distribution of the final scores of the GCP over Antarctica

5.5 GCPs Radiometric quality performance

The following radiometric performance indicators are detailed in the Validation Report [VAL-L1B-L1C-GCP] and are not repeated in this document:

- ✓ First order integrated gradient,
- ✓ Shannon entropy,
- ✓ Cloud, snow and water percentage in GCP chips.

6. User Guide

In this chapter we illustrate some examples of applications using the L1B & L1C GCP GRI.

6.1 Recommendations of use

To use all the points in a statistic way

The more the better. One should favour the use all the GCPs when possible, to improve the quality of the estimated correlation and the accuracy of the n measured spatial offsets.

To respect ranges of use for sensor resolution

The recommendation for sensor resolution to use the GCP DB is from 5 to 30 m and up to 50m in degraded conditions.

Spectral range must fit B04 Sentinel 2 band including its spectral response.

6.2 Examples of use

6.2.1 Use of the L1C GCP GRI by the Sentinel-2 Level-1 processor

The use of the L1C GCP by the Sentinel-2 Level-1 processor is not currently operational but is studied and proven to be as good as (if not better) the Multi-Layer L1B GRI which is currently used in operation.

It can be decomposed in several steps:

- ✓ Find all GCP that are under the processed Datastrip (which will have its geometric model refined) and keep only those that are not in the L1B QUALIT mask (Cloud, Saturation, Degradation).
- ✓ Project those GCP's chips in the L1B geometry of the processed Datastrip.
- ✓ Compute shifts by correlation between GCP's chips resampled and the current Datastrip radiometry. If several chips are available for a GCP, the mean of the shifts found is kept. If the correlation (and curvature) found during the correlation process are under thresholds, the GCP is not kept
- ✓ Once all shifts are computed, filter to have a homogenous spreading and keep a coherent number of shifts.
- ✓ Apply a spatial-triangulation to refine the geometric model based on the shifts computed on GCP.

The parameters computed by the refining part are then used during the orthorectification process to enhance the global geolocation based on the GRI and especially the spatial coregistration between datastrips acquired at different time/from different orbits.

6.2.2 Estimation of the geometrical accuracy of S2 (or other sensors images)

The GCP database, with its accurate geometric performances, can be used to estimate the accuracy of the S2 products. As an example, we estimated the geometric performances of S2 over Europe using 34 different tiles and 211 images using the L1C GCP GRI.

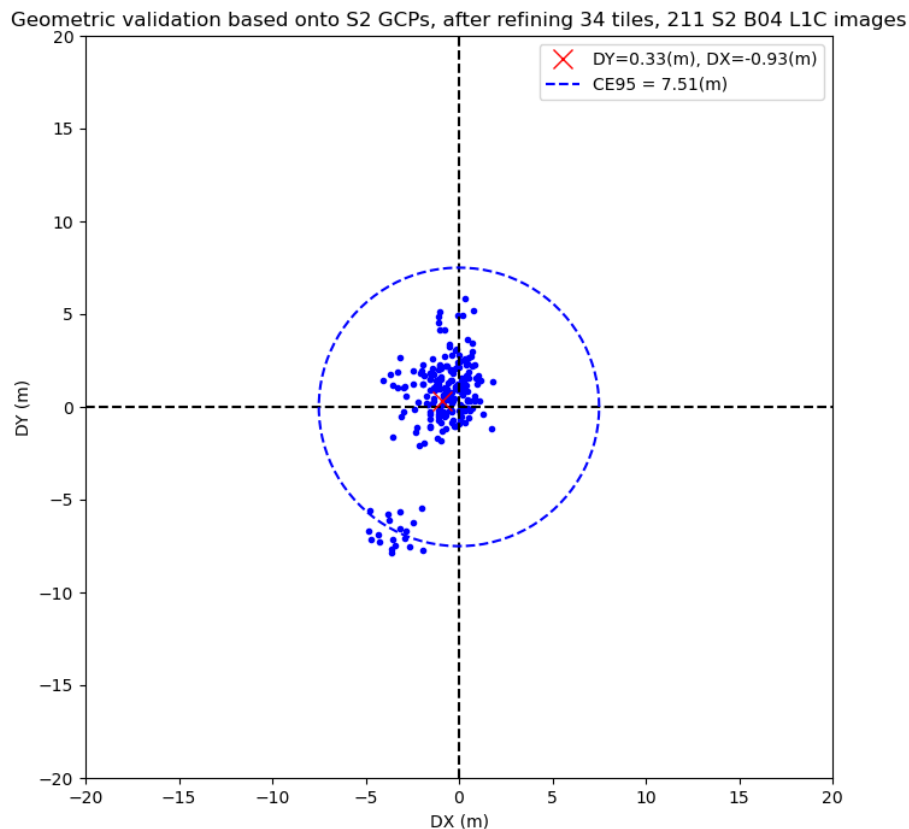


Figure 52: Estimation of the geometric accuracy of S2 using the L1C GCP GRI over Europe.

Synthesis table

The geometric validation results based onto the L1C GCP GRI are the following (non-refined products removed):

Table 5: Summary of the 34 S2 L1C tiles' geometric validation against the L1C GCP GRI

Nb of used S2 tiles	Mean DX (m)	Mean DY (m)	CE95 (m)
34	-0.69	0.96	3.88

7. Distribution, License, and Copyrights

7.1 Distribution

Both L1B and L1C GCPs DB are hosted on a dedicated website available via Sentinel-Online.

They can be downloaded and publicly distributed to the international user community. The Product Handbook and the Validation Report are also made available to the public on the dedicated pages.

7.2 License and copyrights

The L1B & L1C GCP GRI are distributed under Creative Commons Zero (CC0) license.

Under this license, users can copy, modify, distribute, and work with the GCP GRI, even for commercial purposes, all without asking permission.

You can find details about this license here:

- ✓ Summary: <https://creativecommons.org/publicdomain/zero/1.0/deed.en>
- ✓ Complete: <https://creativecommons.org/publicdomain/zero/1.0/legalcode>

End of Document